HIGHWAY RESEARCH RECORD

Number 379

Cement-Stabilized Soil

6 reports
prepared for the
51st Annual Meeting

Subject Areas

62 Foundations (Soils)
63 Mechanics (Earth Mass)

HIGHWAY RESEARCH BOARD
DIVISION OF ENGINEERING NATIONAL RESEARCH COUNCIL
NATIONAL ACADEMY OF SCIENCES—NATIONAL ACADEMY OF ENGINEERING

Washington, D.C. 1972

HIGHWAY RESEARCH RECORD 379

Page 52, the text table should read:

Property	Value
Specific gravity	2.70
Atterberg limits, percent	
Liquid limit	21
Plastic limit	NP
Textural composition, percent	
Gravel, 3 in. to 2.00 mm	20.5
Sand, 2.00 to 0.074 mm	29.5
Silt, 0.074 to 0.005 mm	46.0
Clay, <0.005 mm	4.0
AASHO classification	A-4(3)

NOTICE

The studies reported herein were not undertaken under the aegis of the National Academy of Sciences or the National Research Council. The papers report research work of the authors done at the institution named by the authors. The papers were offered to the Highway Research Board of the National Research Council for publication and are published herein in the interest of the dissemination of information from research, one of the major functions of the HRB.

Before publication, each paper was reviewed by members of the HRB committee named as its sponsor and was accepted as objective, useful, and suitable for publication by NRC. The members of the committee were selected for their individual scholarly competence and judgment, with due consideration for the balance and breadth of disciplines. Responsibility for the publication of these reports rests with the sponsoring committee; however, the opinions and conclusions expressed in the reports are those of the individual authors and not necessarily those of the sponsoring committee, the HRB, or the NRC.

Although these reports are not submitted for approval to the Academy membership or to the Council of the Academy, each report is reviewed and processed according to procedures established and monitored by the Academy's Report Review Committee.

ISBN 0-309-01994-X

Price: $2.20

Available from

Highway Research Board
National Academy of Sciences
2101 Constitution Avenue, N.W.
Washington, D.C. 20418

CONTENTS

FOREWORD

Using natural earth materials in roadways not only conserves resources but also produces economies in construction. Because natural soil is so variable, investigation and development of ways to stabilize the soil have been continuing activities. This RECORD presents the results of studies on cement treatment of earth materials and will be of interest to researchers in the soil-stabilization field and to design and construction engineers as well. Yedavally and Anderson present a simplified design method for the stabilization of Alberta sands. The method shortens testing time and permits adjustment during construction when new materials are disclosed. Dempsey and Thompson demonstrate the effects of "frost-action" parameters in a laboratory freeze-thaw durability test and conclude that the cycling of freezing should be only that necessary to obtain complete specimen freezing and that the number of test cycles should be related to the geographic location and the position of stabilized layer in the pavement system. Wang and Huston; Fossberg, Mitchell, and Monismith; and Chiang and Chae all deal with stresses and strains in a cement-stabilized soil. Wang, Moultrop, and Nacci describe the performance of test pavements in studies to evaluate the usefulness of soil cement in bases and subbases.

SIMPLIFIED SOIL-CEMENT MIX DESIGN METHOD FOR ALBERTA SANDS

Somayajulu P. Yedavally and K. O. Anderson, University of Alberta, Edmonton

Because the conventional procedures for soil-cement mix design are usually quite time-consuming, a simplified method utilizing both 7-day unconfined compressive strength and freeze-thaw loss is proposed. The method is based on an analysis of mix design data collected on more than 100 sources of sand found in Alberta and used for soil-cement base construction. Unconfined compressive strength and freeze-thaw loss at 7 days, tested according to local procedures, have been related to cement requirements for various sands by use of granulometric and density considerations. Least squares fit and linear regression methods have enabled charts to be prepared indicating cement requirements for desired levels of unconfined compressive strength and freeze-thaw losses for various density ranges. The charts developed are considered useful for initial selection of cement requirements for various sands or for adjustments during construction. Although the analysis has been based on local data, more widespread application may be possible.

•CONVENTIONAL laboratory techniques following AASHO, ASTM, or PCA procedures for the mix design of soil-cement are widely used all over the world. Those techniques are modified depending on the climatic conditions and other relevant factors of the locality. The large amount of mix design data accumulated and the experience gained through years with the use of soil-cement could make it possible to derive short-cut methods such as those proposed by PCA (1) or more recently by Kemahlioglu, Higgins, and Adam (2). These methods help in cutting down the normal testing time. Because the methods are derived from statistical analysis of the data of standard procedures, they could be expected to be fairly reliable for the particular local circumstances. The simplified method proposed in this paper is one such method.

Although construction of soil-cement bases was initiated in Alberta in 1953, only since 1959 has construction taken place on a larger scale. Between 1959 and 1968, about 800 two-lane miles of this type of pavement were built on the provincial highway system. Primarily the extensive use of soil-cement base construction in Alberta has been brought about by the depletion of available gravel sources used in standard base construction and the extension of highway surfacing into regions that are void of suitable gravels (3). Large deposits of sand, for use in place of gravel, are available throughout many parts of the province and the utilization of these sand deposits provides substantial savings in haul costs.

Conventional procedures of ASTM and AASHO for soil-cement mix design are generally used with certain modifications. Experience with the sandy soils in Alberta reveals that the wet-dry test does not govern the cement factor and, therefore, is not included in the design procedure. The freeze-thaw test is considered to be a governing criterion for cement content of soil-cement mixes. The effects of freeze-thaw on soil-cement specimens were compared by molding 2 sets of specimens at varying cement contents and at optimum moisture and maximum standard Proctor density. That is, 9 specimens were formed for "control" compressive strengths and were broken after 7 days of curing in ideal moist conditions. The remaining 9 specimens were subjected to 12 freeze-thaw cycles after 7 days of curing in ideal moist conditions. A freeze-thaw cycle was a period of 24 hours at a constant temperature of -10 F, during which the specimens were permitted to absorb water through the base they were set on, and a period of 23 hours at a

temperature of 70 F and 100 percent humidity. The freeze-thaw specimens were brushed by means of a calibrated wire brush only after the final cycle (this is not in accordance with standard ASTM procedures). Generally, 2 to 3 percent of loss due to freezing was considered acceptable. The percentage of loss was computed by determining the quantity of material brushed from the specimens and calculating as a percentage of the dry weight of the specimen.

An extensive evaluation and testing program has been conducted by the Department of Highways and by the Alberta Cooperative Highway Research Program since inception of this type of construction within the province. Design data consisting of the sand source pit numbers, gradations, cement contents, compressive strengths (psi at 7 days, at 28 days, and after 7 days of freeze-thaw), average density (lb/ft^3), and freeze-thaw loss (percent) are available for each of the mix designs.

An analysis has been made of the design data of more than 100 sand sources so that design charts, could be prepared and used to estimate the cement requirements of any sand in the province for stabilization. Such charts permit realistic adjustments to the construction cement contents without much field testing (4). The analysis was made on granulometric and on density considerations.

GRANULOMETRIC CONSIDERATIONS

The grain size characteristics of the sands were determined with a sieve series in which the diameters of successively smaller sieve openings decreased by one-half. The relative surface area per unit weight of spherical particles having the same specific gravity varied inversely with the diameter of the particles. Therefore, the surface area per gram of sand retained within a given sieve interval of the sieve series may conveniently be assumed to be double that of the previous coarser sieve interval. The grading modulus was calculated from the sum of the products of the percentage of the weight retained in each sieve interval and the corresponding surface area factor, divided by 100.

Larnach (5) has shown that the unconfined compressive strengths developed by a sand stabilized with portland cement may be defined by Feret's strength law:

$$S = A(C/V)^N$$

where S is the unconfined compressive strength psi, A is essentially the strength of the cement but is influenced by material and packing, C is the absolute volume of cement, V is the absolute volume of voids in the sand, and N is a constant depending on material and geometrical factors. Hutchinson (6) attempted a graphical model of shear strength development and based it on triaxial tests carried out on 11 sands. His analysis indicated that the factor N was related to the grading modulus GM by the relationship $N = 3.373 - 1.131 \log_{10} GM$, and the factor A, presumably dependent also on cement type and curing environment, was related by $A = 1{,}054\ N^{2.341}$.

In this study the representative soil-cement design data from 100 sand sources were arranged into various groups of grading modulus at a regular interval of 5. In these data, the unconfined compressive strengths developed by each sand at 7 days can be defined by Feret's equation that was fitted to the experimental data for each sand according to the least squares criterion. The values obtained for A and N did not seem to have any trend with respect to the grading modulus of the sand.

The compressive strength values at 7 days and the corresponding C/V values of all sands lying in a grading modulus range were fitted by the least squares criterion, and the A and N values for groups together with correlation coefficients are given in Table 1. Even now, careful examination of the tabulated values shows that the values of neither N nor A indicated any definite trend with respect to the grading modulus. However, by least squares fit, the values of A and N were related by $A = 3{,}626\ N^{2.82}$ with a correlation coefficient of 0.9736. Contrary to what was reported by Hutchinson, N and GM were not related at all.

The erratic behavior of A and N with respect to the grading modulus may be explained as follows: In Feret's strength law, A is defined as essentially the strength of the cement but as being influenced by the material and packing. Grading modulus, obviously, does not reflect either of these characteristics. N is said to be a constant depending on material and geometrical factors. It is doubtful whether the grading modulus takes care of the geometrical factors like shape, surface texture, and so on. Therefore, the granulometric properties of the sands, as defined in terms of the grading modulus, are not satisfactory. The grading modulus is not a clear reflection even of the grading of a material because of the weightage factors given for the different sieves. According to the definition, grading modulus is highly susceptible to the percentage of materials passing sieves No. 50, No. 100, and No. 200 inasmuch as the weightage factors for those sieves are high. A low grading modulus may only mean coarse aggregate, and a high GM may mean more of finer fractions. A well-graded material will have an intermediate value of GM. Two different materials having the same GM may not have the same grading. Therefore, GM that is not truly representative of the gradation cannot be a satisfactory criterion for assessing the development of unconfined compressive strength of soil-cement mixtures.

DENSITY CONSIDERATIONS

Housel (7), Catton (8), Felt (9), and many other investigators have shown that maximum density of soil-cement is a significant factor in the design and performance of soil-cement construction, and it is also generally accepted that a densely compacted material has necessarily high compressive strength. Housel further stated that the consistent relation between density and mechanical analysis is yet another important factor. Variation in texture and grading is quite accurately reflected in the compacted density that gives a measure of the total void content in the mix. The variation in the density can be assessed from a comparison between the ideal gradings and the actual grading, and this is facilitated by the BPR gradation chart (10). (Numerous plots have been prepared and are included in another report (4) but not in this paper.) The BPR chart enables the plotting of the gradations of the different sands and provides at the same time a comparison with the theoretical maximum density grading corresponding to the particular maximum size of the particle of the sand under consideration. The sands that have their gradations farther away from the maximum density line result in low densities; those that lie nearest give high densities. These plots clarify further the fact that the grading modulus does not reflect either the grading or the density.

With the thought that, rather than the GM, the density obtainable with a particular sand would be a more reliable reflection of the grading, we regrouped the soil-cement data on the basis of density ranges.

Relation Between Unconfined Compressive Strength and C/V Values

The 7-day unconfined compressive strength values and the corresponding C/V values of all sands lying in a density range were fitted by least squares criterion, and the A and N values for groups together with the correlation coefficients are given in Table 2. In 5 groups out of the 7 density groups the value of N has a definite trend with respect to density, whereas in 2 groups it is erratic. A term defined as the logarithm of mean density has been used to relate N to density. For the 5 groups, a relation of the form $N = 8.26 \log_{10}(\text{mean density}) - 15.59$ could be established with a correlation coefficient of 0.9750, a standard error of 0.0436, and a modified standard error of 0.0563. The 5 pairs of values of A and N were related by least squares criterion that resulted in the equation $A = 3{,}672\ N^{2.77}$ with a correlation coefficient of 0.9798, a standard error of 1,066, and a modified standard error of 1,376. These 2 relationships were combined to prepare a graphical model (Fig. 1) relating the unconfined compressive strengths to values of C/V for various densities.

Table 1. Unconfined compressive strength and C/V values based on grading modulus.

Group	GM Range	Sand Source Numbers in Group	Group Values N	Group Values A	Number of Data Points	Coefficient of Correlation
1	7.6 to 12.5	23, 121, 123, 159, 77, 46	1.060	3,511	18	0.6383
2	12.6 to 17.5	61, 107, 55, 80, 103, 29, 122, 125	1.376	6,277	24	0.6253
3	17.6 to 22.5	101, 89, 203, 64, 62, 99, 106, 69	1.637	14,668	29	0.8599
4	22.6 to 27.5	49, 91, 160, 32, 114, 35, 120	2.302	43,987	21	0.8014
5	27.6 to 32.5	96, 22, 119, 124, 118, 78, 116, 72, 100, 141, 82	1.644	15,282	36	0.9605
6	32.6 to 37.5	47, 63, 93, 95, 108, 145, 53, 71, 41, 75, 102, 204, 28, 143, 140	1.339	7,186	50	0.8540
7	37.6 to 42.5	81, 43, 110, 115, 92, 60, 166, 87, 147, 67, 88, 83, 57, 74, 76	1.398	9,116	46	0.8814
8	42.6 to 47.5	48, 34, 207, 79, 56, 149, 54, 36, 84, 65, 50, 112	1.596	14,932	41	0.9630
9	47.6 to 52.5	70, 94, 33, 90, 104, 44	1.276	6,379	25	0.8879
10	52.6 to 57.5	109, 113, 86, 105, 66	1.099	4,713	17	0.8553
11	57.6 to 62.5	68, 45, 155, 30, 42	1.488	9,753	16	0.9744
12	62.6 to 67.5	97	0.8450	2,618	3	0.9929
13	67.6 to 72.5	167, 209, 152, 206	0.8670	3,261	13	0.9137
14	72.6 to 77.5	40, 117, 39	1.223	6,719	10	0.9337
15	77.6 to 82.5	98, 85	1.143	4,920	6	0.9796
16	92.6 to 97.5	38	1.667	20,112	3	0.9999

Table 2. Unconfined compressive strength and C/V values based on density.

Group	Density Range	Sand Source Numbers in Group	Group Values N	Group Values A	Log Mean Density	Number of Data Points	Coefficient of Correlation
1	101 to 105	54, 95, 167	0.9870	3,858	2.0128	11	0.8902
2	106 to 110	33, 38, 40, 57, 85, 94, 105, 155, 206	1.2260	6,341	2.0334	31	0.9060
3	111 to 115	28, 30, 32, 35, 36, 39, 42, 44, 50, 53, 77, 86, 89, 91, 97, 98, 104, 106, 113, 117, 143, 152, 204, 207	1.4350	8,582	2.0531	75	0.6989
4	116 to 120	23, 34, 43, 45, 48, 49, 60, 63, 64, 65, 67, 68, 69, 71, 72, 74, 75, 76, 79, 80, 81, 88, 90, 92, 99, 102, 103, 118, 119, 124, 140, 141, 145, 147, 160, 209	1.5660	11,663	2.0719	122	0.8176
5	121 to 125	29, 46, 47, 55, 61, 66, 70, 83, 84, 87, 93, 96, 100, 109, 110, 112, 114, 115, 116, 120, 166	1.1670	5,112	2.0899	71	0.6894
6	126 to 130	22, 56, 62, 78, 82, 101, 159	1.7830	21,579	2.1072	23	0.9809
7	131 to 135	41, 107, 108, 121, 122, 123, 125, 203	1.3790	10,163	2.1239	25	0.9327

The strength values are higher for low density than for high density groups for the same value of C/V, up to C/V values of 0.14 to 0.15. For C/V values beyond 0.15, the higher the density is, the greater is the compressive strength for the same value of C/V. The trend is more and more distinct with increasing values of C/V. This can be explained by the fact that the factor C/V takes care of both cement content and density of a soil-cement mixture. The percentage of cement content is higher in low density groups than in high density groups at the same value of C/V and, hence, the strength is higher. (The variation in the density with cement is assumed to be negligible in this connection.)

Relation Between Unconfined Compressive Strength and Cement Content

In the previous analysis, it is clear that C/V covers the 2 variables in a soil-cement mix, namely, cement content and density. Because all the data had been grouped by density ranges, a study of the direct relationship of strength to the cement content seemed appropiate. Coefficients were computed by linear regression for the relation between 7-day unconfined compressive strength and the cement content and are given in Table 3. A design chart was prepared (Fig. 2) that relates the unconfined compressive strength with the cement content for various density ranges. For low density ranges, particularly from 100 to 115 lb/ft^3, the increase in strength with increase of cement content is not significant, whereas the variation is more significant for density ranges from 115 to 125 lb/ft^3. In the high density range of 125 to 135 lb/ft^3 the increase in strength for any increase in cement content is highly significant.

Relation Between Freeze-Thaw Loss and Cement Content

Experience with the sandy soils used in Alberta has caused the freeze-thaw test to be a governing criterion for cement content of soil-cement mixes (3). Circeo, Davidson, and David (11) reported that a strong logarithmic relationship was found to exist between the cement content and the freeze-thaw loss of a soil-cement mixture. By correlation, they established that 2 freeze-thaw tests would reveal the logarithmic relationship for any soil type. The data for cement content by weight and freeze-thaw losses for each density range were analyzed by correlation analysis and are given in Table 4. From this analysis, a chart was developed (Fig. 3) relating the cement content and freeze-thaw losses for the different density ranges so that the cement content needed for a specified freeze-thaw loss for any sand producing a particular density could be read. The variation in cement requirements for density ranges from 101 to 125 lb/ft^3 is not very significant.

CEMENT CONTENT REQUIREMENTS OF VARIOUS SANDS

The Portland Cement Association has suggested that a study of the strength data is of particular value in the selection of cement contents for investigation. The Associations handbook states, "generally, a soil-cement mixture having a compressive strength that is approximately 300 lb/in.^{2} or more at 7 days, and is increasing, will pass the wet-dry and freeze-thaw tests satisfactorily" (1). Later research shows that strength requirements may vary from 300 to 800 psi for acceptable durability; however, the cement content for the 300 psi has been determined for comparison purposes.

Dacyszyn (3) stated that generally 2 to 3 percent of freeze-thaw loss is acceptable for soil-cement mix design. Based on these 2 criteria, the cement requirements of the sands analyzed have been taken from charts shown in Figures 2 and 3 and are given in Table 5. The actual recommended average cement contents have also been extracted from designs of the Department of Highways of Alberta (DHA) and are tabulated for comparison. It is observed that the cement requirement from the consideration of freeze-thaw loss is usually more than that needed to produce an unconfined compressive strength of 300 psi at 7 days. The recommended cement contents of the DHA are found to be quite in agreement with those suggested by the charts except in one density range, 131 to 135 lb/ft^3. This was probably due to the fact that the DHA recommendation was for

Figure 1. Strength versus C/V values for different densities.

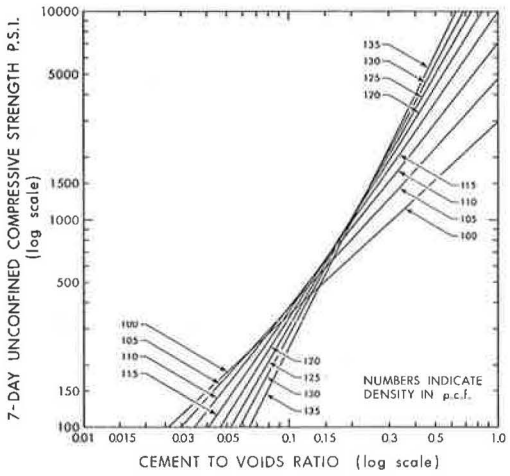

Figure 2. Strength versus cement content for different densities.

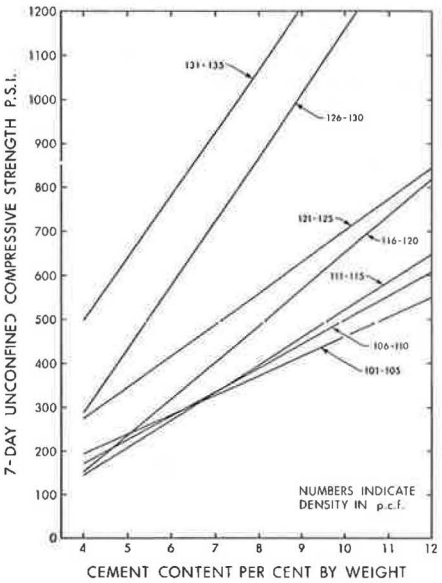

Table 3. Unconfined compressive strength and cement content based on density.

Group	Density Range (lb/ft^3)	Sand Source Numbers in Group	Slope	Intercept	Number of Data Points	Coefficient of Correlation	Coefficient of Determination	Standard Error of Estimate
1	101 to 105	54, 95, 167	44.64	14.19	11	0.8855	0.7830	56.38
2	106 to 110	33, 38, 40, 57, 85, 94, 105, 155, 206	54.93	-48.58	31	0.9187	0.8420	51.65
3	111 to 115	28, 30, 32, 35, 36, 39, 42, 44, 50, 53, 77, 86, 89, 91, 97, 98, 104, 106, 113, 117, 143, 152, 204, 207	62.72	-103.03	75	0.7174	0.5140	118.28
4	116 to 120	23, 34, 43, 45, 48, 49, 60, 63, 64, 65, 67, 68, 69, 71, 72, 74, 75, 76, 79, 80, 81, 88, 90, 99, 102, 103, 118, 119, 124, 140, 141, 145, 147, 149, 160, 209	83.78	-184.46	122	0.8019	0.6430	130.74
5	121 to 125	29, 46, 47, 55, 61, 66, 70, 83, 84, 87, 93, 96, 100, 109, 110, 112, 114, 115, 116, 120, 166	71.83	-14.78	71	0.7174	0.5140	147.03
6	126 to 130	22, 56, 62, 78, 82, 101, 159	145.93	-295.37	23	0.9885	0.9760	49.64
7	131 to 135	41, 107, 108, 121, 122, 123, 125, 203	143.06	-72.54	25	0.8202	0.6720	191.22

Table 4. Freeze-thaw loss and cement content based on density.

Group	Density Range (lb/ft³)	Sand Source Numbers in Group	Slope B	Intercept A	Number of Data Points	Coefficient of Correlation	Coefficient of Determination	Standard Error of Estimate	
								Log C	Cement Content
1	101 to 105	54, 95, 167	-0.2070	0.9430	10	-0.9636	0.9285	0.0360	1.086
2	106 to 110	38, 40, 57, 85, 94, 105, 155, 206	-0.1687	0.9675	27	-0.7758	0.6018	0.0779	1.196
3	111 to 115	28, 30, 32, 35, 36, 39, 42, 44, 50, 53, 77, 86, 89, 91, 97, 98, 104, 106, 113, 117, 143, 152, 204, 207	-0.1951	0.9585	70	-0.8610	0.7413	0.0497	1.121
4	116 to 120	23, 34, 43, 45, 48, 49, 60, 63, 64, 65, 67, 68, 69, 71, 72, 74, 75, 76, 79, 80, 81, 88, 90, 92, 99, 102, 103, 118, 119, 124, 140, 141, 145, 147, 149, 160, 209	-0.2031	0.9148	116	-0.8539	0.7291	0.0619	1.153
5	121 to 125	29, 46, 47, 55, 61, 66, 70, 83, 84, 87, 93, 96, 100, 109, 110, 112, 114, 115, 116, 120, 166	-0.1881	0.8918	66	-0.8237	0.6784	0.0730	1.183
6	126 to 130	22, 56, 62, 78, 82, 101, 159	-0.2561	0.8002	23	-0.8936	0.7985	0.0705	1.176
7	131 to 135	41, 107, 108, 121, 122, 123, 125, 203	-0.2552	0.7487	23	-0.8036	0.6457	0.1139	1.300

Figure 3. Freeze-thaw loss versus cement content for different densities.

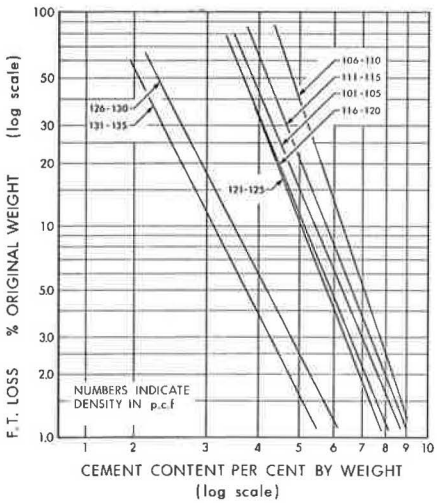

Table 5. Recommended cement content requirements.

Group	Density Range (lb/ft³)	300-psi, 7-Day Compressive Strength	2 to 3 Percent Freeze-Thaw Loss	Average DHA Design
1	101 to 105	6.5	7.0 to 7.7	8.67
2	106 to 110	6.5	7.8 to 8.3	8.2
3	111 to 115	6.5	7.3 to 8.0	8.03
4	116 to 120	5.65	6.6 to 7.2	6.92
5	121 to 125	4.2	6.4 to 6.9	6.41
6	126 to 130	4.1	4.8 to 5.3	5.3
7	131 to 135	under 4	4.3 to 4.75	3.72

cement-treated bases in which case the specification would be less rigorous.

The densities used in the development of the charts are laboratory densities, and, because the cement contents suggested by the charts are based on these, they will be valid only in case the field densities are almost the same as laboratory densities; otherwise, the cement contents have to be adjusted to the density attained.

USE OF THE CHARTS AND THEIR LIMITATIONS

For any particular sand, if the laboratory density can be determined, the cement content required for a specified permissible freeze-thaw loss can be determined from the chart shown in Figure 3. The unconfined compressive strength that is expected to be developed can be read out from the chart shown in Figure 2 at the cement content indicated earlier. Thus, the charts could enable realistic adjustments to the construction cement contents without much field testing in the event of major changes in grading developing.

Although the analysis has been based on actual mix design data of the Department of Highways of Alberta and can be considered to be a reliable guide for quick field adjustments, it has certain limitations. Anderegg (12), in discussing the factors affecting the development of compressive strength, stated that the amount of cement hydrated, the properties of the aggregate including especially the surface condition, the workability of the mix, and the keying effect of the large particles are all factors important in the order cited. Felt (9) stated that sandy soils, too, may react differently with cement depending on their chemical makeup and surface chemical properties. Another important factor that has pronounced influence on the physical properties of soil-cement mixtures is the water added. Because some of these factors could not be considered in the analysis, the charts developed have their limitations.

CONCLUSIONS

The following conclusions have been drawn from this study:

1. The grading modulus of a sand is not a reliable criterion for the design of soil-cement mixes;
2. The sand density attainable provides a useful parameter for estimating the cement requirements for various sands;
3. The BPR gradation chart gives a comparative assessment of the density attainable with a particular sand, when the gradation of the sand is plotted on the chart;
4. The charts developed from the analysis contained in this paper are useful for quick adjustments of the construction cement contents without much field testing, are particularly useful for the Alberta sands, and may have general application even for other areas if similar charts are developed; and
5. The use of this method results in a decrease in testing time to about 2 days, which is only the time needed for the Proctor density tests on the sand concerned.

ACKNOWLEDGMENTS

This paper is based on soil-cement mix design data collected for a project of the Alberta Cooperative Highway Research Program sponsored by the Department of Highways of Alberta, the Research Council of Alberta, and the Department of Civil Engineering of the University of Alberta. Special acknowledgment is due B. P. Shields for his helpful suggestions and for making data available for analysis.

REFERENCES

1. Soil-Cement Laboratory Handbook. Portland Cement Association, 1959.
2. Kemahlioglu, A., Higgins, C. M., and Adam, V. A Rapid Method for Soil-Cement Design: Louisiana Slope Value Method. Highway Research Record 198, 1967, pp. 19-29.
3. Dacyszyn, J. M. Soil-Cement Construction in Alberta. Proc., 42nd Conv. of Canadian Good Roads Assn., Sept. 1961.
4. Yedavally, S. P., and Anderson, K. O. Analysis of Soil-Cement Mix Design. Dept. of Civil Eng., Univ. of Alberta, Edmonton, Prel. Rept., Jan. 1971.

5. Larnach, W. J. Relationship Between Dry Density, Voids/Cement Ratio, and the Strength of Soil Cement Mixtures. Civil Engineering and Public Works Review, Vol. 55, No. 648, July 1960.
6. Hutchinson, B. G. Granulometric Properties of Cement Stabilized Sands. Jour. Soil Mech. and Found. Div., Proc. ASCE, Vol. 89, No. SM3, Part 1, May 1963.
7. Housel, W. S. Experimental Soil-Cement Stabilization at Cheboygan, Michigan. HRB Proc., Vol. 17, Part 2, 1937, pp. 46-66.
8. Catton, M. D. Basic Principles of Soil-Cement Mixtures and Exploratory Laboratory Results, HRB Proc. Vol. 17, Part 2, 1937, pp. 7-31.
9. Felt, E. J. Factors Influencing Physical Properties of Soil-Cement Mixtures. HRB Bull. 108, 1955, pp. 138-163.
10. Goode, J. F. A New Graphical Chart for Evaluating Aggregate Gradation. U.S. Bureau of Public Roads, 1962.
11. Circeo, L. J., Davidson, D. T., and David, H. T. Relationship Between Cement Content and Freeze-Thaw Loss of Soil-Cement Mixtures. Highway Research Record 36, 1963, pp. 133-145.
12. Anderegg, F. O. Grading Aggregates II—The Application of Mathematical Formulas to Mortars. Industrial and Engineering Chemistry, Vol. 23, No. 9, Sept. 1931.

EFFECTS OF FREEZE-THAW PARAMETERS ON THE DURABILITY OF STABILIZED MATERIALS

Barry J. Dempsey and Marshall R. Thompson,
Department of Civil Engineering, University of Illinois

A study was conducted to evaluate the effects of various frost-action parameters on the freeze-thaw durability of stabilized materials and to determine which parameters could be modified so that a characteristic freeze-thaw cycle could be adapted to laboratory use. The parameters studied were cooling rate, freezing temperature, length of freezing period, and thawing temperature. The cooling rate was found to be an important factor affecting the freeze-thaw durability of stabilized soils. Lower cooling rates (0.2 to 2.0 F/hr) that correlated best with quantitative field data were generally the most detrimental to durability. A sustained freezing study revealed that the length of the freezing period did not have to be greater than that required to accomplish complete freezing of the test specimen. The study further indicated that freezing and thawing temperatures should be representative of those for in-service pavement systems. Thawing temperatures for some stabilized materials are important because strength increase caused by a pozzolanic reaction is possible at high temperatures. The number of cycles used in a laboratory freeze-thaw test should be related to geographical location, climatic conditions, and position of the stabilized layer in the pavement system. For Illinois climatic conditions, a laboratory freeze-thaw cycle representative of field conditions would require a completion period of 48 hours.

•STABILIZED materials such as soil-cement, lime-fly ash, and lime-soil mixtures are used extensively as base and subbase layers in pavement construction. In areas where frost action occurs, these materials must retain their integrity and maintain adequate residual strength at all times in order to provide adequate structural performance.

The laboratory testing procedure used to evaluate the freeze-thaw durability of stabilized soils and materials should be representative of field conditions. In an effort to develop a rational durability testing procedure, Thompson and Dempsey (1) used a pavement heat-transfer model to generate quantitative data for describing frost action in pavement systems.

A characteristic freeze-thaw cycle for central Illinois is shown in Figure 1 and includes all of the important frost-action parameters as follows: cooling rate, freezing temperature, length of freezing period, warming rate, thawing temperature, length of thawing period, and number of freeze-thaw cycles. Illinois frost-action parameter data (1) showed substantial variability as related to the effects of geographical location, climate, and position in the pavement system.

When an accelerated freeze-thaw durability test is developed, it may be desirable to change some of the frost-action parameters so that the period of time to complete a freeze-thaw cycle can be shortened for laboratory use. However, any changes made in the cycle should not substantially alter its representation of the frost action that actually occurs in field pavement systems.

The purpose of this study was to evaluate the effects of various frost-action parameters on the freeze-thaw durability of stabilized materials and to determine which parameters can be modified so that the characteristic field frost-action cycle can be adapted to laboratory use.

PREPARATION OF TEST SPECIMENS

Materials

The frost-action parameter study was limited to 2 typical Illinois soils that can be effectively stabilized with various stabilizing agents. These soils included Illinoian till and Ridgeville fine sandy loam. Table 1 gives the natural properties of the soils used in the parameter study. A hydrated high calcium lime containing 96 percent available $Ca(OH)_2$ with 95 percent passing the No. 325 sieve was used to stabilize the Illinoian till. A Type 1 portland cement was used to treat the Ridgeville fine sandy loam.

Mixture Design

Currently recognized strength and freeze-thaw durability testing procedures were utilized to establish the mixture designs. The amount of lime added to the Illinoian till consisted of the optimum percentage (dry-weight basis) determined from previous strength studies by Thompson (2). The soil-cement was prepared and tested according to AASHO T135 and T136 procedures, and Portland Cement Association criteria were employed to establish the design cement content for the Ridgeville fine sandy loam. Table 1 gives the specimen sizes, curing periods, mixture designs, and density properties for the stabilized materials used in this study.

Compaction Procedures

All freeze-thaw test specimens were molded in 2-in. diameter by 4-in. steel molds in 3 equal layers. Each layer was scarified to ensure bonding between the layers. The compaction hammer had a 2-in. diameter base, and the compactive effort was applied by a 4-lb weight falling freely through a distance of 12 in. The compactive efforts for the lime- and cement-stabilized materials were established to produce average densities equivalent to those obtained by AASHO T99 compaction procedures.

Curing Procedures

Immediately after compaction, the test specimens were removed from the molds, marked, and weighed. The lime-soil specimens were cured in sealed plastic bags for 48 hours at 120 F. The soil-cement specimens were cured for 7 days in a room having a relative humidity of 100 percent and a temperature of 77 F. The accelerated curing periods used in the laboratory have generally been found to approximate field curing.

FREEZE-THAW TESTING PROCEDURE

The parameter study was conducted with a specially designed freeze-thaw durability testing unit that can be programmed to accurately control both the top and the bottom temperatures on a specimen. Either closed- or open-system moisture conditions can be provided. A more detailed discussion of the testing unit can be found in previous work by Dempsey (3).

In the parameter study the freeze-thaw test consisted of a combination of open and closed conditions depending on whether the free water near the base of the specimens was in a frozen or an unfrozen condition. The test specimens were supported on ½-in. porous stones that were in contact with the free water surface.

The freezing gradient in the test specimens was one dimensional and proceeded from the top to the bottom during freezing. A temperature differential between the top and bottom of the 4-in. specimens was maintained at approximately 3 F in all of the test series, based on the results of pavement heat-transfer model studies of typical Illinois pavements.

The freeze-thaw cycle programmed into the testing unit was variable depending on the frost-action parameter being investigated. Cooling rates of 0.2, 0.5, 1.0, 2.0, 5.0, and 10.0 F/hr were studied. The cooling rate was defined as the rate of temperature change at the surface of the test specimens. The minimum freezing temperatures were 25 F for the 0.2 F/hr cooling rate and 18 F for the remaining cooling rates. The time required for the temperature to cool from 30 F to the minimum freezing temperature

Figure 1. Characteristic frost-action cycle for central Illinois.

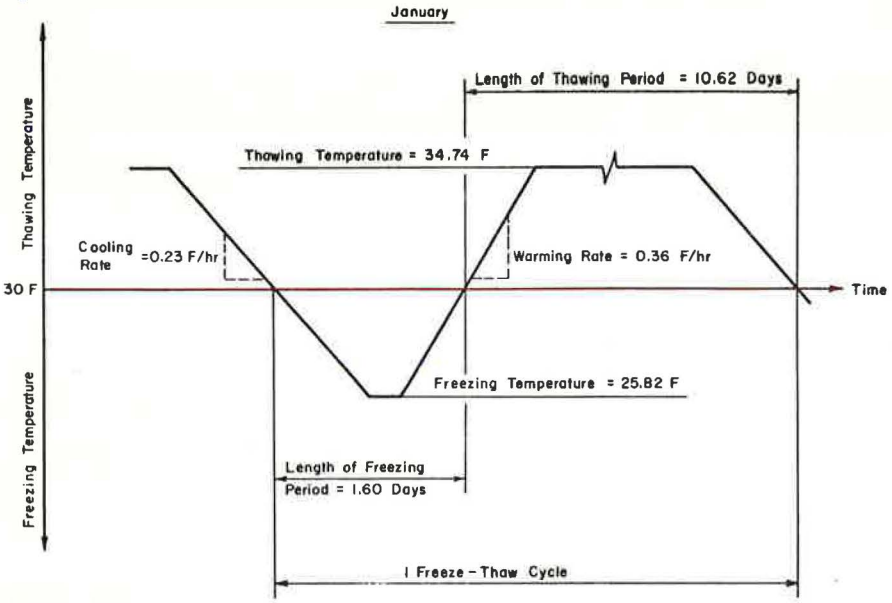

Table 1. Natural and mixture properties of samples.

Property	Illinoian Till	Ridgeville Fine Sandy Loam
Natural Properties		
Location	Sangamon County	Iroquois County
Description	Calcareous loam till of Illinoian age	B-horizon of profile developed in fine sandy outwash material
AASHO classification	A-4(4)	A-4(1)
Atterberg limits		
Liquid limit, percent	21	25
Plasticity index, percent	6	7
<200 sieve, percent	57	37
<2-μ clay, percent	18	17
Mixture properties		
Specimen size, in.	2 by 4	2 by 4
Stabilization agent	lime	cement
Content, percent	3	8
Curing	48 hours at 120 F sealed	7 days at 77 F in 100 percent relative humidity
Dry density, lb/ft^3	121.0	114.8
Water content, percent	13.0	14.3

ranged from a maximum of 24 hours for the slowest cooling rates (0.2 F/hr and 0.5 F/hr) to approximately 1 hour for the fastest cooling rate (10 F/hr). The freezing period lasted about 30 hours for the slowest cooling rates and 12 hours for the fastest cooling rate. A warming rate of 2 F/hr was used in all of the tests. The thawing temperature was set at 40 F. The length of time to complete 1 freeze-thaw cycle in the laboratory varied between 24 and 48 hours. A maximum of 6 freeze-thaw cycles was considered sufficient to determine whether there was a significant influence of a particular parameter.

At the end of the sixth freeze-thaw cycle a freezing duration study was conducted. A sustained freezing period of 96 hours was used to determine whether prolonged freezing influenced the durability of stabilized materials.

EVALUATION METHODS AND TEST DATA

Unconfined compressive strength change, moisture content change, and unit length change were used to assess the freeze-thaw durability of the stabilized materials during cyclic freezing and thawing and sustained freezing. Generally, evaluation tests were conducted on specimens at the end of 3 and 6 freeze-thaw cycles and specimens subjected to sustained freezing for periods of 48 or 96 hours after the sixth freeze-thaw cycle.

The average values for the data collected from the freeze-thaw parameter study are given in Table 2. The data listed are for 2 stabilized mixtures that were subjected to different freeze-thaw environments.

Unconfined Compressive Strength Change

Changes in unconfined compressive strength were determined by testing 4 specimens at various times during the freeze-thaw period. Specimens tested immediately after the cure period (0 freeze-thaw cycles) were used as the reference for determining strength change.

Moisture Content Change

Townsend and Klym (4) and Dempsey and Thompson (5) have indicated that the relative increase in moisture content and moisture distribution in lime-soil mixtures may be related to freeze-thaw durability. The vertical distribution of moisture and the rate of moisture movement in test specimens subjected to one-directional freezing are indicative of permeability and capillarity that can influence heave and associated strength loss. In this study, the effects of freeze-thaw cycles on moisture content changes in the stabilized specimens were analyzed. Moisture content determinations were made for the middle layer of 2 unconfined compressive strength specimens after they had been tested.

Unit Length Change

Length changes in 2 specimens were continuously monitored by use of linear motion potentiometers that had been calibrated to record relative length changes on a strip chart. The total specimen length change was measured to the nearest 0.001 in. The unit length change was determined as the inches of length change per inch of specimen height.

ANALYSIS AND DISCUSSION OF FROST-ACTION PARAMETERS

Earlier studies by Thompson and Dempsey (1) have indicated that cooling rate, freezing temperature, and length of freezing period are the most significant parameters influencing cyclic freeze-thaw deterioration. Kaplar (6) has indicated that the cooling rate is a major factor influencing the rate of heave in soils. Work at the University of Illinois has shown that the thawing temperature is also an important parameter in freeze-thaw durability studies of stabilized materials that gain strength through a pozzolanic reaction.

Frost-action literature generally shows that the number of freeze-thaw cycles has a substantial influence on the durability of pavement materials. In freeze-thaw durability testing it is important that the number of freeze-thaw cycles used be related to the geographical location, climatic conditions, and the depth in the pavement system where the stabilized material is placed.

Cooling Rate

The rate at which a stabilized material cooled during freezing was expected to have considerable influence on freeze-thaw durability. Figure 2 shows the influence of cooling rate on the moisture change, unit length change, and unconfined compressive strength change of soils stabilized with lime and cement after 3 freeze-thaw cycles. Figure 3 shows a similar plot for the stabilized soils after 6 freeze-thaw cycles. The slower cooling rates (0.2 to 2.0 F/hr) generally have the most detrimental influence on freeze-thaw durability. This fact is important because quantitative frost-action data based on heat-transfer model studies (1) show that cooling rates in Illinois generally vary between 0.2 and 1.0 F/hr.

Table 3 gives data from the statistical analyses of the influence of cooling rate on moisture change, unit length change, and unconfined compressive strength change after 3 and 6 freeze-thaw cycles. Moisture change in the middle layer of the lime-soil specimens was significantly influenced ($\alpha = 0.05$) by cooling rate. Although the data were not significantly different, the soil-cement did show substantial moisture increases at the lower cooling rates. Cooling rate did not significantly influence the unit length change in the stabilized soils. However, inspection of the data indicates that cooling rate appears to have some effect on the unit length change. The soil-cement generally experienced greater unit length changes at the lower cooling rates. Unconfined compressive strength change was significantly influenced ($\alpha = 0.05$) by cooling rate. In some cases it would appear that greater strength losses occurred during the slower cooling rates.

The stabilized materials used in the study were designed to be durable mixtures. It is probably for this reason that significant influences of cooling rate were not evident for some of the methods used for evaluating freeze-thaw durability. It is apparent that unconfined compressive strength change was a valid indicator of the freeze-thaw deterioration of these stabilized soils.

Freeze-thaw durability evaluation of stabilized soils and materials has shown that the data are highly variable and the variability tends to increase with the number of freeze-thaw cycles. Unpublished data at the University of Illinois have indicated that the coefficient of variation of unit length change data for a stabilized soil after 6 freeze-thaw cycles often exceeds 20 percent. Similar findings are true for moisture change and unconfined compressive strength change. Because of the substantial variability in freeze-thaw durability evaluation, statistically significant differences are difficult to establish but important qualitative trends can be discerned.

Freezing Temperature

The freezing temperature used in the study ranged from 18 to 25 F depending on the cooling rate. These temperatures are realistic for frost-action analysis in Illinois. It must be emphasized that the magnitude of the freezing temperature is dependent on factors such as geographical location, climatic conditions, pavement composition, and position in the pavement system.

Length of Freezing Period

The length of time that specimens should remain in a frozen condition is an important parameter in the development of an accelerated freeze-thaw test. In this study a sustained 96-hour freezing period was used after the specimens had been frozen for the sixth cycle. It was hypothesized that, once freezing of a specimen had occurred, additional freezing time would not have a detrimental effect on durability.

Table 4 gives the results of a statistical evaluation of the influence of sustained freeze-thaw durability. Unconfined compressive strength change, unit length change,

Figure 2. Effect of cooling rate on moisture change, unit length change, and unconfined compressive strength change after 3 freeze-thaw cycles.

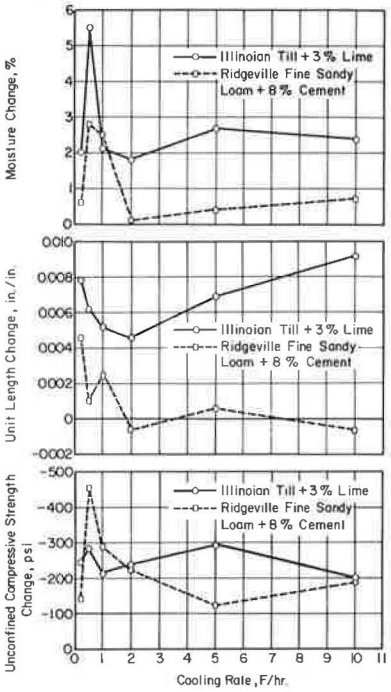

Figure 3. Effect of cooling rate on moisture change, unit length change, and unconfined compressive strength change after 6 freeze-thaw cycles.

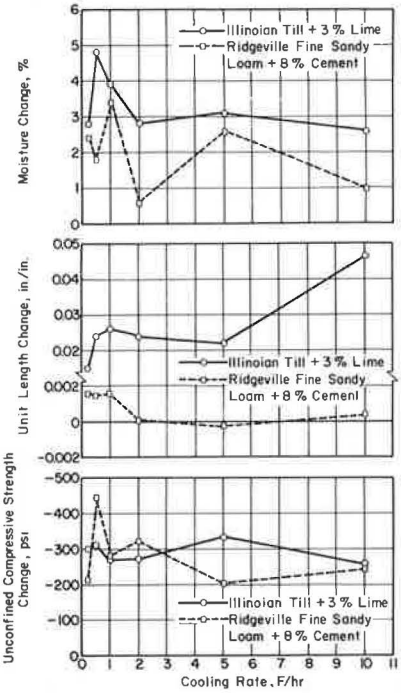

Table 2. Average data for frost-action parameters.

Stabilized Material	Cooling Rate (F/hr)	Unconfined Compressive Strength Change (psi)					Moisture Content Change at Middle Layer (percent)					Unit Length Change (in./in.)			
		Freeze-Thaw Cycles			Hours of Sustained Freezing		Freeze-Thaw Cycles			Hours of Sustained Freezing		Freeze-Thaw Cycles		Hours of Sustained Freezing	
		0	3	6	48	96	0	3	6	48	96	3	6	48	96
Illinois till + lime	0.2	410	166	110	140	140	10.6	12.6	13.4	13.4	13.2	+0.0078	+0.0150	+0.0150	+0.0150
	0.5	386	102	76	103	82	9.7	15.2	14.5	—	—	+0.0062	+0.0237	+0.0231	+0.0231
	1.0	354	141	85	—	—	11.4	13.5	15.3	—	—	+0.0052	+0.0260	—	—
	2.0	382	145	109	—	—	11.2	13.0	14.0	—	—	+0.0046	+0.0232	—	—
	5.0	408	116	74	63	17	10.1	12.8	13.2	14.9	16.1	+0.0069	+0.0221	+0.0425	+0.0554
	10.0	321	122	63	67	63	11.1	13.5	13.7	14.5	13.9	+0.0092	+0.0465	+0.0466	+0.0431
Ridgeville sand + cement	0.2	634	492	421	486	458	12.9	13.5	15.3	16.0	14.1	+0.0046	+0.0016	+0.0016	+0.0004
	0.5	893	438	450	446	489	11.7	14.5	13.5	14.3	14.1	+0.0010	+0.0015	+0.0000	+0.0001
	1.0	704	418	425	—	—	11.7	14.2	15.1	—	—	+0.0025	+0.0016	—	—
	2.0	737	513	415	558	468	12.9	12.8	13.5	14.0	14.7	-0.0006	+0.0001	-0.0001	-0.0001
	.5.0	579	451	376	458	405	12.5	12.9	15.1	16.0	15.0	+0.0006	-0.0002	-0.0015	-0.0005
	10.0	673	388	431	547	514	13.2	14.0	14.2	13.6	14.6	-0.0006	+0.0004	+0.0000	-0.0001

Table 3. Results of statistical analysis of effect of cooling rate.

Evaluation Method	Stabilized Material	Freeze-Thaw Cycles	Test	Cooling Rate (F/hr) 0.2	0.5	1.0	2.0	5.0	10.0	F (calculated)	F (α = 0.05)	Difference[a]
Avg unconfined compressive strength change, psi	Illinois till + lime	3	A[b]	-244	-284	-213	-237	-292	-199	10.15	2.77	Y
			D[c]	-292	-284	-244	-237	-213	-199			
		6	A	-300	-310	-269	-273	-234	-258	10.79	3.03	Y
			D	-334	-310	-300	-273	-269	-258			
	Ridge. sand + cement	3	A	-142	-455	-286	-224	-128	-285	14.60	2.81	Y
			D	-455	-286	-285	-224	-142	-128			
		6	A	-213	-443	-279	-322	-203	-242	7.86	2.81	Y
			D	-443	-322	-279	-242	-213	-203			
Avg moisture content change at middle layer, percent	Illinois till + lime	3	A	+2.0	+5.5	+2.1	+1.8	+2.7	+2.4	77.66	4.39	Y
			D	+5.5	+2.7	+2.4	+2.1	+2.0	+1.8			
		6	A	+2.8	+4.8	+3.9	+2.8	+3.1	+2.6	8.50	4.39	Y
			D	+4.8	+3.9	+3.1	+2.8	+2.8	+2.6			
	Ridge. sand + cement	3	A	+0.6	+2.8	+2.5	-0.1	+0.4	+0.8	3.90	4.39	N
		6	A	+2.4	+1.8	+3.4	+0.6	+2.6	+1.0	1.72	4.39	N
Avg unit length change, in./in.	Illinois till + lime	3	A	+0.0078	+0.0062	+0.0052	+0.0046	+0.0069	+0.0092	1.41	4.39	N
		6	A	+0.0150	+0.0237	+0.0260	+0.0236	+0.0221	+0.0465	3.00	4.39	N
	Ridge. sand + cement	3	A	+0.0046	+0.0010	+0.0025	+0.0006	+0.0006	+0.0006	2.17	4.39	N
		6	A	+0.0016	+0.0015	+0.0016	+0.0001	-0.0002	+0.0004	0.45	4.39	N

[a] N = no significant difference; Y = significant difference. [b] Analysis of variance.
[c] Duncan's multiple range. Any 2 means underscored by same line are not significantly different; any 2 means not underscored by same line are significantly different.

Figure 4. Effect of curing temperature on change in unconfined compressive strength.

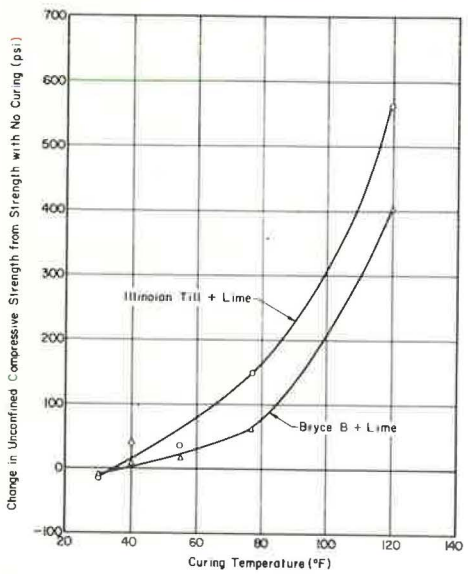

Table 4. Results of statistical analysis of effect of sustained freezing.

Stabilized Material	Evaluation Method	Cooling Rate (F/hr) 0.2	0.5	1.0	2.0	5.0	10.0
Illinois till + lime	Unconfined compressive strength change	N	N	—	—	N	N
	Unit length change	N	N	—	—	Y	N
	Moisture content change at middle layer	N	—	—	—	Y	N
Ridgeville sand + cement	Unconfined compressive strength change	N	N	—	N	N	Y
	Unit length change	N	N	—	N	N	N
	Moisture content change at middle layer	N	N	—	N	N	N

Note: α = 0.05. N = no significant difference; Y = significant difference; and — = no data.

and moisture content change at the end of the sixth freeze-thaw cycle are compared with data for continuous freezing periods of 48 and 96 hours. Regardless of the cooling rate, an increase in the length of the freezing period generally (23 out of 26 cases) did not significantly influence ($\alpha = 0.05$) the freeze-thaw durability of the stabilized materials tested.

Thawing Temperatures

Work by Thompson and Dempsey (1) indicated that thawing temperatures in stabilized materials are considerably lower than those specified in the standard freeze-thaw durability testing procedures. Generally, thawing temperatures ranging from 35 to 45 F are common in Illinois, depending on geographical location, climatic conditions, and depth in the pavement system (1).

The durability of stabilized materials such as lime-soil mixtures and lime-fly ash-aggregate mixtures that gain strength through a pozzolanic reaction can be substantially influenced by the magnitude of the thawing temperature. Figure 4 shows the effect of curing temperature on the change in unconfined compressive strength of 2 reactive soils stabilized with lime. It is shown that strength increases with an increase in curing temperature. At temperatures below approximately 40 F the strength increase with curing time essentially ceases.

If realistic durability evaluation is to be ensured, it is apparent that the thawing temperature used in a freeze-thaw durability test for stabilized materials should be representative of the thawing temperatures in the field.

SUMMARY AND CONCLUSIONS

Frost-action parameters that were expected to influence the development of a laboratory freeze-thaw durability test for stabilized soils and materials were studied. Although the data showed substantial variability, cooling rate was found to be an important factor affecting the freeze-thaw durability of stabilized soils. The lower cooling rates, which correlate best with quantitative field data, were generally the most detrimental to durability.

Data analyses for the frost-action parameter study indicate that a rational laboratory freeze-thaw durability test for typical Illinois climatic conditions should have the following characteristics:

1. A slow cooling rate, possibly between 0.2 and 1.0 F/hr;
2. Freezing and thawing temperatures similar to those of the in-service pavement system;
3. A freezing period not necessarily greater than that required to accomplish complete freezing of the test specimen; and
4. Number of cycles related to geographical location, climatic conditions, and position of the stabilized layer in the pavement system.

The laboratory freeze-thaw cycle now being used to test stabilized materials at the University of Illinois requires 48 hours to complete. This length of time was necessary because it was found that, for Illinois climate, the cooling rate in pavement systems is quite low (approximately 0.25 F/hr). Although the length of time to complete a freeze-thaw cycle is quite long, it is believed that the laboratory testing procedure is representative of field temperature conditions.

ACKNOWLEDGMENTS

This study was conducted as a part of the Illinois Cooperative Highway Research Program by the staff of the Department of Civil Engineering, University of Illinois, under joint sponsorship of the Illinois Division of Highways and the Federal Highway Administration. The opinions, findings, and conclusions expressed in this report are those of the authors and not necessarily those of the Illinois Division of Highways or the Federal Highway Administration.

REFERENCES

1. Thompson, M. R., and Dempsey, B. J. Quantitative Characterization of Cyclic Freezing and Thawing in Stabilized Pavement Materials. Highway Research Record 304, 1970, pp. 38-44.
2. Thompson, M. R. Lime Reactivity of Illinois Soils as It Relates to Compressive Strength. Civil Eng. Studies, Univ. of Illinois, Illinois Coop. Highway Res. Prog. Series NP-4, 1964.
3. Dempsey, B. J. A Programmed Freeze-Thaw Durability Testing Unit for Evaluating Paving Materials. Unpublished, 1971.
4. Townsend, D. L., and Klym, T. W. Durability of Lime-Stabilized Soils. Highway Research Record 139, 1966, pp. 25-41.
5. Dempsey, B. J., and Thompson, M. R. Durability Properties of Lime-Soil Mixtures. Highway Research Record 235, 1968, pp. 61-75.
6. Kaplar, C. W. Phenomenon and Mechanism of Frost Heaving. Highway Research Record 304, 1970, pp. 1-13.

DIRECT-TENSILE STRESS AND STRAIN OF A CEMENT-STABILIZED SOIL

Mian-Chang Wang and Milton T. Huston, University of Rhode Island

A direct-tension test that permits determination of stress and strain is described. An equation for prediction of direct-tensile strength of a cement-stabilized silty soil compacted at standard AASHO optimum moisture content and cured at 70 F in a moist room is given as a function of cement content and curing time. Relations among the direct-tensile strength, unconfined compressive strength, and split-tensile strength for the conditions studied are established. Results show that the strain at failure in compression and tension respectively remains constant as long as dry density, molding moisture content, and curing conditions are the same. The cement-stabilized soil possesses different moduli in tension and compression; the modular ratio is proportional to the strength ratio. Both strength and strain at failure vary significantly with curing temperature; decreasing curing temperature decreases the strength but increases the strain at failure.

•BECAUSE of its inherent appreciable tensile strength, cement-stabilized soil has demonstrated itself as one of the most favorable materials for pavement construction. Development of a rational approach to the design of pavement requires establishment of both strength and failure strain criteria in tension and in compression so that stresses and strains developed in the pavement can be limited within a permissible range.

The importance of the property of stabilized soils under tension has provoked considerable study for years. Most studies (1, 2, 3, 4, 5), however, concentrate on the property of tensile strength determined by using the split-tension test; information on the deformation modulus and failure strain in tension is scarce.

A testing method that permits determination of both tensile stress and strain was developed. The developed testing method was used to study the stress-strain behavior of a cement-stabilized soil under uniaxial tension. This paper describes the test method and test results obtained to date.

TEST METHOD

Providence silt, a common glacial deposit in Rhode Island, was used for study. Classification test results of Providence silt are as follows:

Property	Value
Specific gravity	2.75
Atterberg limits, percent	
Liquid limit	28
Plastic limit	24
Plasticity index	4
Grain size, percent	
0.02 to 2.0 mm	9
0.002 to 0.02 mm	54
Finer than 0.002 mm	37
Classification	
Unified soil system	ML
AASHO system	A-4(8)

The test soil was treated with Type 1 portland cement. Tap water was used for mixing throughout.

The test samples were prepared at an optimum moisture content and a maximum dry density (14.5 percent and 106.5 lb/ft^3 respectively) determined prior to treatment by using the standard AASHO compaction effort. The test specimens were 1¾ in. wide over the central section and 3 in. wide at the ends with a thickness of approximately 1¾ in. (This thickness was chosen to make a square cross section at central portion of the test specimen.) The overall height of the test specimen was 7 in., including one 2-in. midsection, two 1-in. butted ends, and two 1½-in. transition sections connecting the central portion and both ends. Detailed dimension is shown in Figure 1.

The necked-down test specimens were molded in 3 equal layers by using the static compaction method. Each end of the specimen was reinforced in each layer with a steel reinforcement to ensure a rupture at the central portion. The reinforcement was 1/16 in. in diameter and was fabricated to a shape shown in Figure 1. The tip of the reinforcement was 2 in. off midpoint of the test specimen.

The test specimens were clamped on 2 acrylic jaws. The jaws are dimensioned to fit snugly to the ends of the test specimens. The test specimens could, therefore, slide into position very easily. The jaws were connected to the testing machine by using a spherical contact at each joint to provide a better alignment during loading.

Tests were conducted by using a Wykeham Farrance strain rate control machine. A strain rate of 0.050 in./min was used throughout the test. A diaphragm type of load cell was used for determination of applied load, and a pair of linear variable differential transformers (LVDT) was used for measurement of deformation over the central section of the test specimens. Both load and deformation were monitored by using an electronic recorder.

TEST RESULTS AND DISCUSSION

The mode of failure in tension is typical of brittle fracture, although appreciable strains develop before failure occurs (Fig. 2). The rupture plane, in general, is nearly perpendicular to the direction of loading. Figure 2 shows the typical stress-strain relationship in both tension and compression for the test soil treated with 3 percent cement and cured at approximately 70 F in a moist room.

Figure 2 also shows the difference in stress-strain behavior between tension and compression. The test specimens failed at considerably greater stress and strain in compression than in tension; however, the modulus of deformation was considerably higher in tension than in compression. Both tensile and compressive strengths increased significantly with increasing curing time and cement content of the test specimens. The test results accumulated to date suggest that the tensile strength of cement-treated Providence silt compacted and cured at the conditions mentioned can be predicted reasonably well by using the following expression:

$$\sigma = \left\{(1/2) + \left[60\,C^{4/3}/\left(32 + C^{4/3}\right)\right]\right\}\left\{1 + \left[2\,\log^{8/3} t/\left(2 + \log^{8/3} t\right)\right]\right\} \qquad (1)$$

where

σ = direct tensile strength, psi,
c = cement content by weight of solid, percent, and
t = curing time, days.

A correlation between the direct-tensile strength and the unconfined compressive strength of the test soil is shown in Figure 3. The unconfined compressive strength was determined from 1.4-in. diameter specimens. The tensile-to-compressive strength ratio varies approximately from 10 to 20 percent increasing with an increase in the compressive strength for the conditions studied.

Tensile strength of the test soil was also determined by using the split-tension test. The split-tension test specimens had a diameter of 3 in. and a height of 2 in. and were tested at a rate of loading equal to that of the direct-tension test. Figure 4 shows a comparison between direct- and split-tensile strengths. The direct-tensile strength is approximately 15 percent higher than the split-tensile strength.

Figure 1. Test setup.

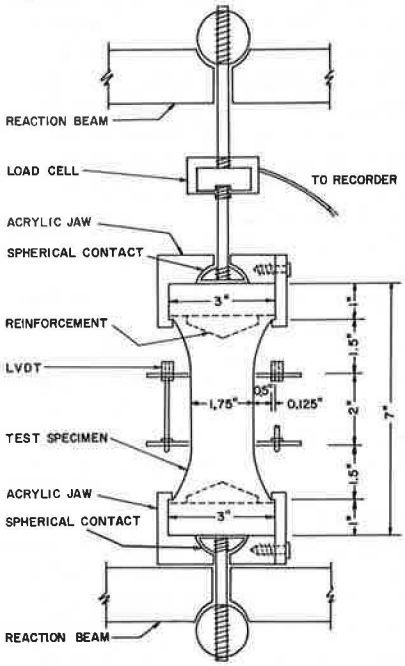

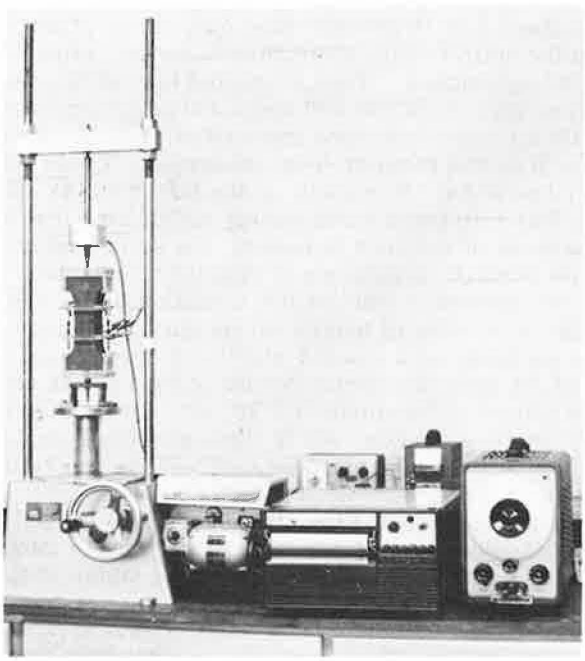

Figure 2. Stress-strain relation of 3 percent cement-treated Providence silt.

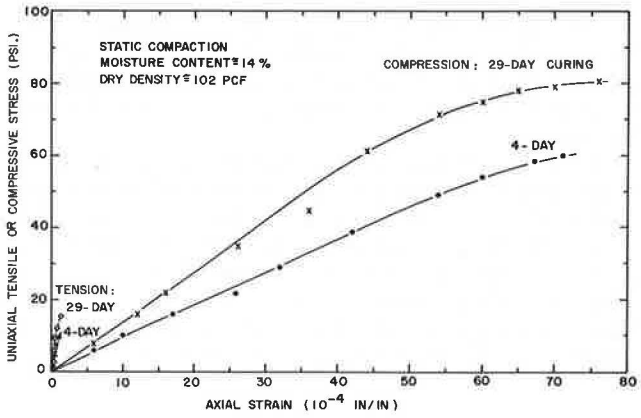

Figure 3. Relation of direct-tensile strength and unconfined compressive strength.

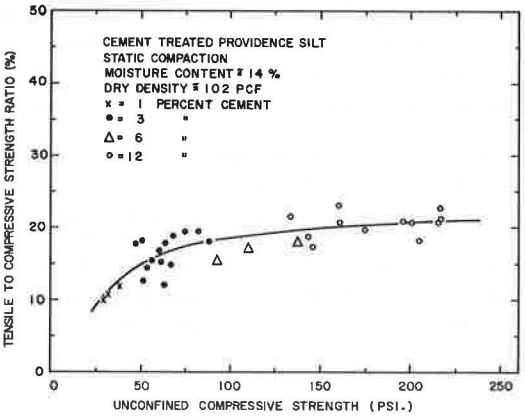

The ratio of split-tensile to unconfined compressive strength (Figs. 3 and 4) ranges from about 9 to 18 percent depending on the strength level. Kennedy et al. (5) correlated the split-tensile strength with the unconfined compressive strength of cement-treated aggregates. They suggested that within the range of conditions studied, viz., between approximately 500 and 2,000 psi unconfined compressive strength, the split-tensile strength increased from about 14 to 16 percent of the unconfined compressive strength as the strength level increased. These results are reasonably close to the upper boundary, 18 percent, of the test results. The materials studied by Kennedy et al. had a strength considerably higher than that of the material used in this study.

Because of the ease in testing, the split-tension test is often used for evaluating the tensile strength properties of stabilized materials. However, the split-tension test does not provide a test-loading condition to resemble that in the field, nor does it permit determination of tensile strain during loading. In addition, Adepegba (6) concluded, from his study on a cement-stabilized laterite and a cement-stabilized sand, that the stabilized soils can easily deform at load points and that such deformations are usually large enough to invalidate $\sigma = 2P/\pi dt$, the formula normally used for calculating the split-tensile strength. All of these constitute disadvantages and, therefore, restrict the application of the split-tension test for determination of tensile-strength property of stabilized soils.

Figure 5 shows that the strain at failure ranged between 0.9 and 1.5×10^{-4} in./in. in tension and between 60 and 90×10^{-4} in./in. in compression. Cement content and curing time had essentially no influence on the strain at failure. The tensile strain at failure is approximately 1.0 to 2.5 percent of compressive strain for all cement contents and all curing times studied. The compressive strain at failure for cement-treated silty clay, reported by Wang et al. (7), ranged from 80 to 100×10^{-4} in./in. regardless of change in cement content (from 3 to 6 percent), curing age, and effect of repeated loading and a 1.3-hour delay in compaction. They also reported that the flexural strain at failure for the same material ranged between 3 and 5×10^{-4} in./in. independent of the factors studied. The compressive strain at failure coincides surprisingly well. It appears that the strain at failure in tension and compression respectively remains constant as long as the dry density, molding moisture content, and curing conditions are the same.

Although the strain at failure remains constant with respect to the curing time and cement content, the increase in strength with increasing curing time and cement content would cause an increase in the initial tangent modulus of deformation. Figure 6 shows the variation of initial tangent modulus with the strength in both tension and compression. The test results suggest that the modulus is directly proportional to the strength with a proportional factor approximately 12,000 and 185 respectively for tension and compression. Based on these 2 factors, the modular ratio can be expressed in terms of the strength ratio as follows:

$$\frac{\text{tensile modulus}}{\text{compressive modulus}} \cong 65 \times \frac{\text{direct-tensile strength}}{\text{unconfined compressive strength}} \qquad (2)$$

where the strength ratio is a function of strength level as shown in Figure 3.

The modulus of deformation is one of the basic factors required in pavement stress and strain analysis. Figures 3 and 6 provide data sufficient for evaluation of both tensile and compressive moduli from the unconfined compressive strength for the soil studied.

Equation 2 indicates that the cement-stabilized soil possesses different moduli in tension and compression, except when the tensile strength equals approximately 1.5 percent of the compressive strength. According to data shown in Figure 4, the strength ratio varies from 10 to 20 percent and, therefore, the tensile modulus ranges between 650 and 1,300 percent of the compressive modulus. It would appear, therefore, necessary to treat the cement-stabilized soil as a material with moduli that are different in tension and compression in the analysis of stress and strain in cement-stabilized soil pavements.

Figure 4. Relation of direct-tensile strength and split-tensile strength.

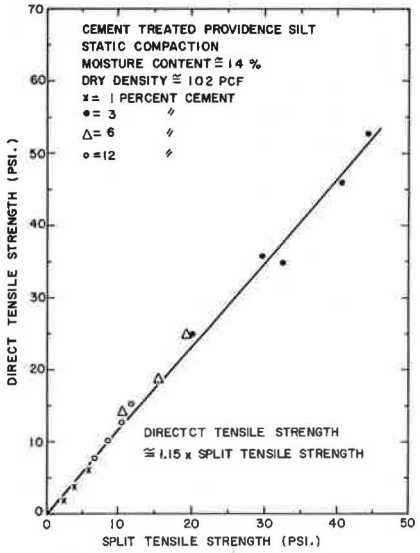

Figure 5. Strain at failure as a function of curing time.

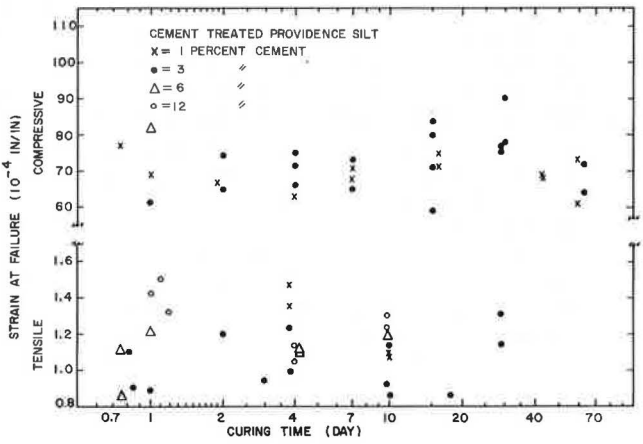

Figure 6. Initial tangent modulus as a function of strength in both tension and compression.

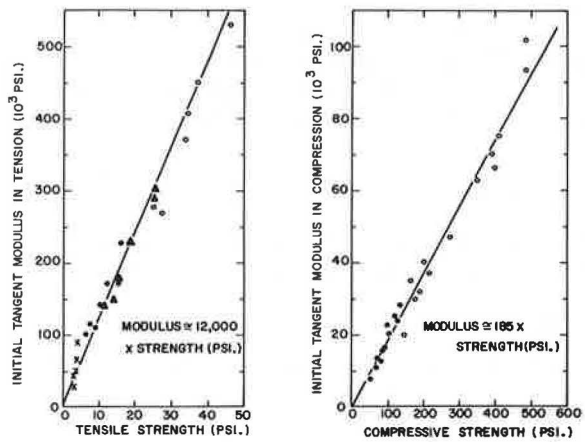

Figure 7. Effect of curing temperature on strength and failure strain in both tension and compression.

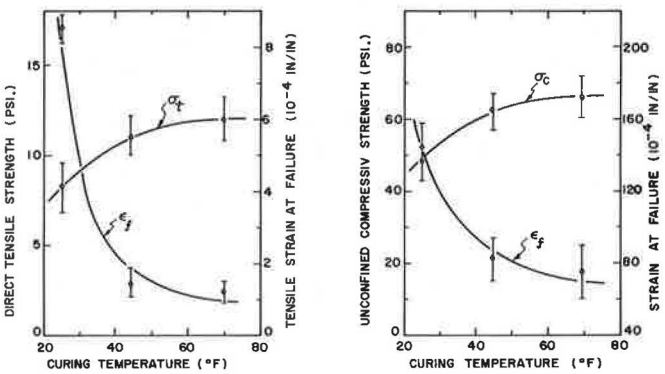

All preceding test results were established for the test specimens wrapped and cured at approximately 70 F in a moist room. The influence of curing temperature on the tensile strength property was studied by wrapping the soil specimens compacted to identical conditions and curing them at temperatures of 25 and 45 F. The test results (Fig. 7) indicate that decreasing curing temperature decreases the strength but increases the strain at failure probably because of the retardation of cement hydration at low temperature. The same effect of curing temperature on the compressive and tensile strength of lime-treated material was obtained respectively by Ruff and Ho (8) and Moore et al. (4).

Test results would imply that, if a representative field-strength property of cement-stabilized soils is obtained, the test specimens used in the laboratory study should be cured at the same temperature as that which occurs in the field. Furthermore, selection of strength and failure strain criteria for a design of cement-stabilized soil pavements requires consideration of the effect of ambient temperature.

SUMMARY AND CONCLUSIONS

A testing method that permits determination of both stress and strain during the course of uniaxial tension was described. A study of the direct-tensile stress and strain behavior of cement-stabilized Providence silt leads to the following conclusions:

1. The mode of failure in tension is typical of brittle fracture although appreciable strains develop before failure;
2. Both strength and failure strain in tension are considerably smaller than those in compression (for the conditions outlined, the direct-tensile strength of the test soil ranges approximately from 10 to 20 percent of the unconfined compressive strength, and the failure strain in tension ranges between 1.0 and 2.5 percent of that in compression for all cement contents and curing times studied);
3. The cement-stabilized soil possesses different moduli in tension and in compression, and the modular ratio is directly proportional to the strength ratio; and
4. Decreasing curing temperature decreases the strength but increases the failure strain in both tension and compression.

ACKNOWLEDGMENTS

The authors are grateful to Wen-hsiung Chen for conducting the testing program and to Kuo-Yang Lee for assistance in the testing and the preparation of the drawings.

REFERENCES

1. Thompson, M. R. Split-Tensile Strength of Lime-Stabilized Soils. Highway Research Record 92, 1965, pp. 69-82.
2. Kennedy, T. W., and Hudson, W. R. Application of Indirect Tensile Test to Stabilized Materials. Highway Research Record 235, 1968, pp. 36-48.
3. Moore, R. K., Kennedy, T. W., and Hudson, W. R. Factors Affecting the Tensile P Properties of Cement-Treated Materials. Highway Research Record 315, 1970, pp. 64-80.
4. Moore, R. K., Kennedy, T. W., and Kozuh, J. A. Tensile Properties for the Design of Lime-Treated Materials. Highway Research Record 351, 1971, pp. 78-86.
5. Kennedy, T. W., Moore, R. K., and Anagnos, J. N. Estimations of Indirect Tensile Strengths for Cement-Treated Materials. Highway Research Record 351, 1971, pp. 112-114.
6. Adepegba, D. A Test for Validity of Indirect Tension Tests of Stabilized Soils. Jour. of Materials, Vol. 6, No. 3, Sept. 1971, pp. 555-575.
7. Wang, M. C., Mitchell, J. K., and Monismith, C. L. Stresses and Deflections in Cement-Stabilized Pavements. Univ. of California, Berkeley, Contract Rept. 3-145, Sept. 1969.
8. Ruff, C. G., and Ho, C. Time-Temperature Strength-Reaction Product Relationships in Lime-Bentonite-Water Mixtures. Highway Research Record 139, 1966, pp. 42-60.

CRACKING AND EDGE-LOADING EFFECTS ON STRESSES AND DEFLECTIONS IN A SOIL-CEMENT PAVEMENT

Per E. Fossberg, International Bank for Reconstruction and Development; and James K. Mitchell and Carl L. Monismith,
Institute of Transportation and Traffic Engineering, University of California, Berkeley

Two 8½-in. thick panels of stiff soil-cement base were constructed on a soft clay subgrade, and one of them was loaded to crack. Both pavements were then tested in repeated loading, unsurfaced and surfaced with 1, 3, and 5 in. of asphalt concrete. Deflections, stresses, and strains under loading were recorded and compared. Vertical deflections were greater by about 20 percent, and subgrade stresses directly under the load were greater by at least 50 percent in the cracked section than in the uncracked pavement. Cracking had a large influence on horizontal strains near the crack in the base but had only a small influence on strains in the asphalt concrete surfacing. A saw-cut was made through the uncracked pavement surfaced with 5 in. of asphalt concrete, and repeated plate-load tests were done with the plate center 24 and 8 in. from the cut. Loading at 24 in. had negligible effects on vertical deflections but increased subgrade stresses near the cut by about 40 percent. Loading at 8 in. increased vertical deflections by at least 60 percent and subgrade stresses near the cut by about 100 percent. Laboratory-determined values for the elastic properties of the clay, the soil-cement, and the asphalt concrete and the various assumed loading conditions were used as input for computer predictions of stresses and deflections. Very satisfactory agreement was obtained between the predicted and measured stresses and deflections.

•EXPERIENCE and theoretical investigations have shown that most soil-cement pavements are subject to cracking due to shrinkage stresses during curing, traffic loadings, and temperature stresses. Although it has long been realized that cracking in soil-cement bases is likely to be the rule rather than the exception, recent studies have been aimed at the explanation of crack development, and some study has been made of techniques for minimizing crack formation (2, 3, 4). Little is known, however, about the relative performance of cracked and uncracked soil-cement slabs under load.

During a recent investigation at the University of California, Berkeley (1), the opportunity arose to carry out field measurements of stresses and deformations associated with edge loading and cracking of a soil-cement pavement. A recently developed finite-element program, capable of 3-dimensional analysis (5, 7), provided a tool for analytical treatment of the problem and thus allowed for correlation to be drawn between field measurements and theoretical analysis.

This paper gives an outline of the study, reports on field test results, describes the method of analysis, compares the results of the theoretical analyses with field data, and draws conclusions relative to the design and performance of soil-cement pavements.

OUTLINE OF STUDY

Two panels of soil-cement base (cement-treated granular material meeting Portland Cement Association's criteria for wet-dry and freeze-thaw testing) were constructed, each approximately 8.5 in. thick and 20 ft square in plan on top of a natural clay subgrade. Classification properties of the subgrade clay are as follows:

Property	Value
Yellow plastic clay	
Water content, percent	18 to 30
Liquid limit, percent	56
Plasticity index, percent	34
Dry density, lb/ft^3	92 to 102
CBR	2 to 5
Unconfined compressive strength, psi	10 to 50

A cement content of 5.5 percent and well-graded gravel with fines were used in the soil-cement as follows:

Sieve Size	Percent Finer by Weight
¾ in.	100
No. 4	62
No. 16	39
No. 50	25
No. 200	17

One of the two pavement sections was loaded until it cracked. On top of the base, 5 in. of asphalt concrete surfacing was constructed in 3 lifts, permitting determination of the influence of asphalt concrete thickness on the performance of the pavement sections with both cracked (pavement 1) and uncracked (pavement 2) soil-cement base.

Repeated-load plate tests (20 load applications per minute of 0.1-sec duration) were carried out. On the subgrade, plate diameters of 24 in. and 30 in. with pressures up to 5 psi were used. On the soil-cement base and the successive lifts of asphalt concrete, the plate sizes ranged from 8 to 24 in. in diameter with plate pressures from 2.5 to 150 psi, depending on plate size. For each repeated-load plate test, vertical deflections at the pavement surface, at the surfacing-base and base-subgrade interfaces, and at various depths into the subgrade were measured. Vertical stresses and horizontal strains were measured at various locations in the subgrade, soil-cement base, and asphalt concrete surfacing of both pavement structures. Figure 1 shows the location of the gauges in the pavement structure. A complete description of the instrumentation and test procedures is given elsewhere (1).

As a final test on the uncracked pavement, after the full 5 in. of asphalt concrete had been placed and the load tests completed, the pavement was cut with a diamond saw over its full length and full depth of surfacing and base. Repeated-loading tests were then carried out with the center of the plate 24 in. (position A, Fig. 1) and 8 in. (position B) from the cut. This arrangement permitted study of edge loading in an instrumented part of the pavement. Figure 1 shows the position of the saw cut in pavement 2 and the position of the crack in pavement 1.

Laboratory tests were used to ascertain the elasticity and strength characteristics of the pavement materials. The tests were done on cylindrical samples of undisturbed subgrade clay, on soil-cement beams, on cylinders and prisms prepared in the laboratory or cut from the test pavements, and on beams and prisms of asphalt concrete also cut from the test pavements. A triaxial apparatus, allowing for independent application of axial and radial stresses, was used to test the clay and soil-cement cylinders. For the subgrade cylinders and some of the soil-cement specimens, strains were recorded with linear variable differential transformers (LVDT); for the asphalt concrete and other soil-cement specimens, bonded strain gauges were utilized. For all tests, the load frequency and duration were the same as those used for the repeated-load plate tests on the prototype pavements.

Laboratory data used in the theoretical analyses were determined to correspond to the appropriate field conditions, e.g., subgrade moisture content, soil-cement curing

time, and asphalt concrete temperature. On this basis the following values were selected (Fig. 2):

1. The subgrade was nearly saturated but with water content varying with depth as shown in Figure 2, Poisson's ratio was assumed to be 0.48, and the elastic modulus varied between 1,600 and 18,000 psi;
2. Field testing was started on the soil-cement base approximately 6 weeks after construction at which time the elastic modulus had reached a relatively constant value of 2,800,000 psi and Poisson's ratio was determined to be 0.16; and
3. The asphalt concrete temperature was comparatively uniform—65 F—for all the field tests at which Poisson's ratio was taken to be 0.35 and the elastic modulus was 350,000 psi.

FIELD TEST RESULTS

Cracking of Soil-Cement Base

On the basis of recorded tangential and radial strains in the base, it was postulated that the position of the crack caused by overloading was approximately as shown in Figure 1. Figure 3a shows the radial strains close to the top (gauge 2-6) and the bottom (gauge 2-8) of the unsurfaced soil-cement slab and at a horizontal distance of 3 in. from the center of the load plotted as a function of plate load and pressure. For the 8-in. diameter plate, the load-strain relationship recorded on gauge 2-8 was close to linear and of about the same magnitude as found for the uncracked slab. For the 12-in. and 16-in. diameter plates, however, a drastic increase in strains was recorded on gauge 2-8, indicating cracking under the 12-in. plate load. (After cracking had occurred the "strain" recorded on the LVDT type of strain gauge mainly reflects the gap at the crack. Thus, a recorded strain of 160×10^{-6} on a gauge where the anchor plates are 2 in. apart represents a gap of about 320×10^{-6} in.)

The plate size appears to be of little significance for the induced strain, the determining factor being plate load. Gauge 2-6 showed that, for the 12-in. diameter plate, tensile strains occurred even at a depth of $1\frac{1}{2}$ in. below the top of the pavement. This may be taken as a further indication of the position of the crack.

The data shown in Figure 3a have been replotted in terms of a profile through the soil-cement slab (Fig. 4). The large difference in strains at the bottom of the base, as recorded under the 8-in. diameter plate (base uncracked) and the 12-and 16-in. diameter plates (base cracked), is evident.

Figure 3b shows tangential strains close to the top (gauge 2-5) and the bottom (gauge 2-7) of the soil-cement slab, 6 in. from the center of the load, and in a direction nearly parallel to the apparent direction of the crack. From the load-strain patterns observed for the 8-in. diameter plate (compression near top, tension near bottom), zero tangential strains would occur about midheight in the uncracked slab. For the cracked slab, in the direction of gauges 2-5 and 2-7, the data for the 12-and 16-in. diameter plates show that this pattern remains essentially unchanged, although the strains are somewhat larger for the cracked slab. Had the slab remained uncracked for the 12-in. and 16-in. diameter test plates, the strains should have been somewhat less than those recorded for the 8-in. plate for a given plate load. The data shown in Figure 3b indicate that the strains in the positions of gauges 2-5 and 2-7 have increased by at least 20 percent because of the cracking. This increase is important because the tensile stresses at the bottom of the slab, near the crack, and in a direction parallel to it may be critical for the propagation of further load-associated cracking.

Vertical deflections under repeated loading are shown in Figure 5. For the 8-in. diameter test plate, when the slab was not cracked, the load-deflection relation is close to that shown for the uncracked slab. However, for the cracked slab subjected to repeated loading on 12- and 16-in. diameter plates, deflections are increased. Based on argument in the preceding paragraph, Figure 5 shows that cracking of the pavement causes an increase in deflection of at least 20 percent. The increases postulated for tangential strains at positions 2-5 and 2-7, and for the vertical deflections, are thus in a agreement.

Figure 1. Positions of stress and strain gauges, crack and pavement cut, and loads A and B.

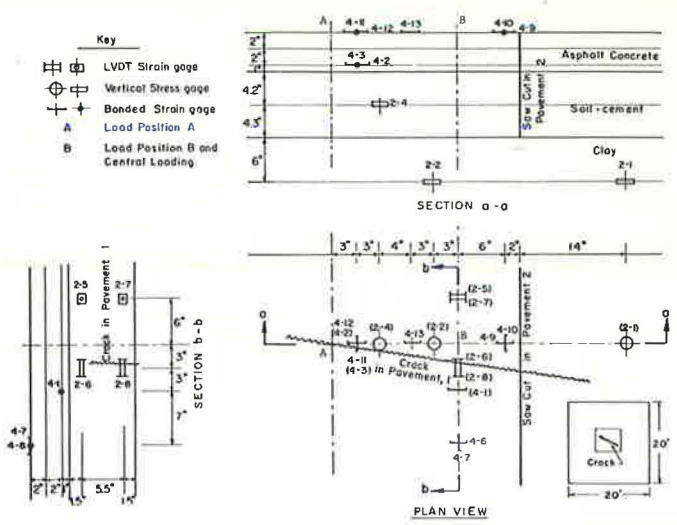

Figure 2. Property values used for structural analysis of pavement.

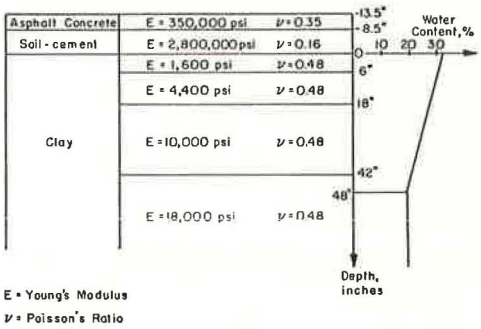

Figure 3. Resilient strains under repeated loading of unsurfaced, cracked soil-cement pavement near top and bottom.

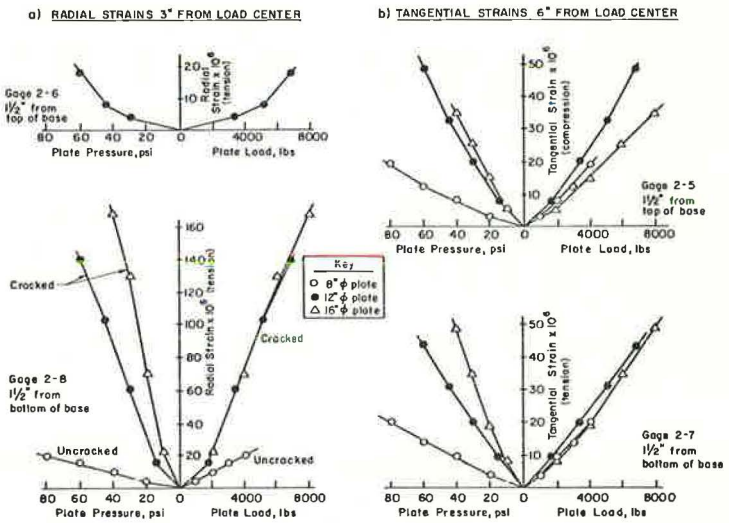

Figure 4. Resilient radial strains under repeated loading of unsurfaced, cracked soil-cement pavement at 3-in. distance from center of load.

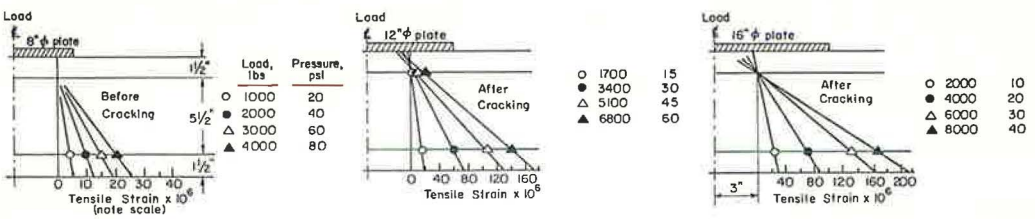

Figure 6 shows the vertical stresses obtained for gauges 2-1 and 2-2 installed 6 in. beneath the top of the subgrade and at horizontal distances of 22 and 3 in. respectively from the center of the loaded area. It will be noted that for gauge 2-1 the stresses were of the same magnitude as reported for the uncracked slab. For gauge 2-2, however, which was situated close to the center of the load and presumably close to the crack, the cracking seemed to have a more profound effect. Although the stresses before cracking (8-in. diameter test plate) are about equal to those obtained for the uncracked slab, cracking caused a sharp increase in stress at the position of gauge 2-2. It appears that the subgrade stresses near the crack increased by at least 50 percent as a result of cracking of the slab, based on the values recorded for the 12- and 16-in. diameter plates.

For both the cracked and the uncracked pavements, the provision of 5 in. of asphalt concrete surfacing reduced the base deflection and subgrade stresses by only about 20 percent. This relatively small effect can probably be attributed to the fact that the asphalt concrete in this experiment had a stiffness only about one-eighth of that of the soil-cement. The asphalt concrete had, however, a large effect in reducing the vertical stresses at mid-depth in the base. Cracking of the base had a large influence on horizontal strains near the crack in the base but had only a small influence on strains in the asphalt concrete surfacing.

Edge Loading

Repeated loading was carried out on the sawed pavement by using 8-, 12-, and 18-in. diameter plates with the centers located 24 and 8 in. from the cut (load positions A and B respectively shown in Fig. 1). The saw cut was made near the end of the test program after tests were made of the completed pavement structure containing a 5-in. thick asphalt concrete surfacing.

Figure 7 shows the deflection patterns under a 12-in. diameter plate at load positions A and B. Although the deflection was considerably increased when the loading was close to the edge, the difference is accounted for mainly in the deformation of the upper 1 ft of the subgrade. For load position A, the maximum deflection occurred under the load and not at the edge. This is contrary to what one might have expected, considering the high stiffness of the soil-cement base. An interesting observation is that the soil-cement slab on the other side of the cut also deflected somewhat. There is no doubt that the saw cut extended right through the pavement; hence, the observed deflection of the adjacent slab must have been due to the subgrade "pulling" it down. This again was unexpected in view of the high slab stiffness and the absence of load transfer across the cut.

The deflections of the base course under the center of the load, as functions of plate size, pressure, and load are shown in Figure 8 for load positions A and B. In both cases, the deflections were closely related to the plate load, irrespective of plate size, a finding in agreement with the cases of central loading of the slab. Conversely, the deflections increased rapidly with plate size for any given pressure intensity on the plate. Loading at position A gave deflections only slightly larger than those at central loading, and loading at position B gave deflections at least 50 percent larger. A tentative conclusion is, therefore, that for a soil-cement pavement loading 2 ft or more from the edge can be treated as central loading and loading very close to the edge may cause considerably larger deflections and also higher stresses and strains in the base.

Figure 9a shows the stresses in the clay subgrade (gauge 2-2) as a function of the plate size, pressure, and load for test position A; Figure 9b shows the same data for test position B. As in the case of deflections, the stresses in both cases were uniquely related to the plate load, irrespective of plate size. A comparison of these load-stress diagrams with values for central loading shows that the stresses obtained by central loading were increased by approximately 40 percent and 100 percent for load positions A and B respectively.

Figure 10 shows the load-strain data for 4 of the 10 gauges positioned on top of the various asphalt concrete lifts. In these diagrams, the full and dashed lines represent load positions A and B respectively. In the following, some of the most significant aspects will be discussed.

Figure 5. Resilient vertical deflections as function of plate size, plate pressure, and plate load for cracked and uncracked pavements.

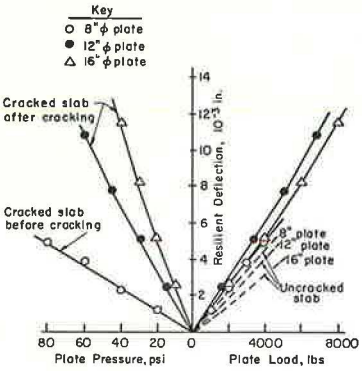

Figure 6. Vertical stresses at 6-in. depth into subgrade.

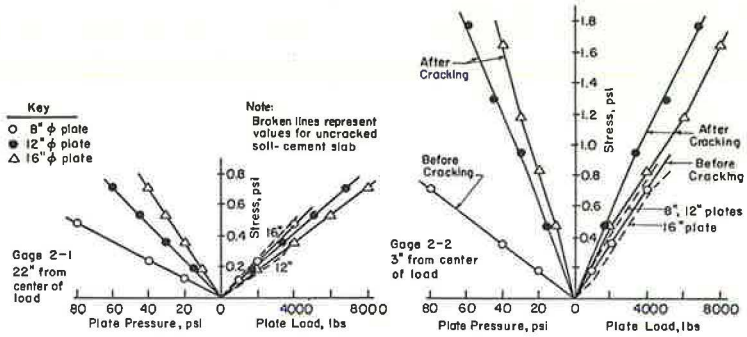

Figure 7. Effect of curing temperature on strength and failure strain in both tension and compression.

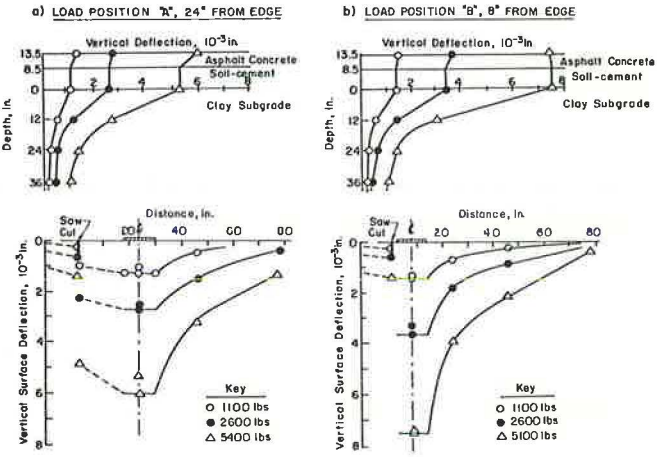

Figure 8. Resilient vertical deflections at top of soil-cement base under repeated loading on edge of pavement with 5-in. asphalt concrete surfacing.

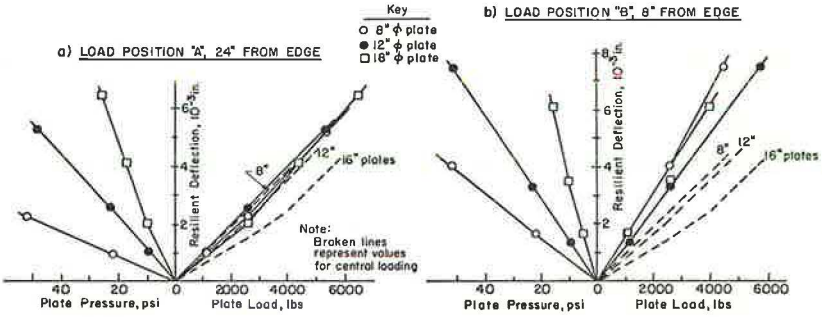

Figure 9. Vertical stresses in subgrade under repeated loading on edge of pavement with 5-in. asphalt concrete surfacing.

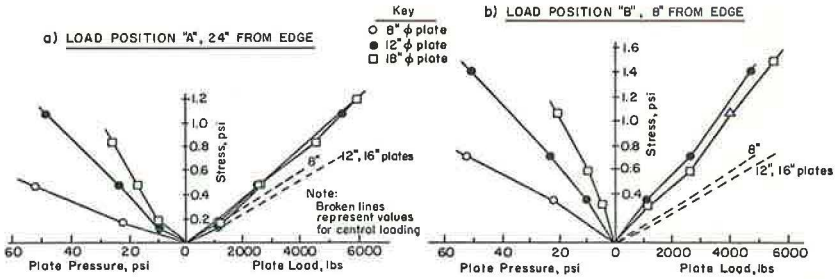

On gauge 4-1 compressive strains were observed when the load was at position A. Good agreement is obtained between these strains and those obtained in the central loading case for gauge 4-2 in about the same position relative to the load. (The inflection points of the deflection basin under central loading of this pavement system lie on a circle with a radius of approximately 2 ft. Thus, for loading 2 ft from the edge, which is position A, strains recorded in the vicinity of the load should be comparable with those obtained in the central loading case.) In the present case, the strains are relatively little affected by the plate size. From the geometry of the loading (Fig. 1) it is entirely logical that relatively large tensile strains should be recorded on this gauge when the load is at position B. The data shown in Figure 10 indicate that this is correct. Although the changes in strains from compression to tension, depending on load position, are important when fatigue is considered, the stresses resulting from the strains here encountered are not critical for the asphalt concrete.

On gauge 4-3, with the load at position A, relatively small compressive strains were recorded for the 12- and 18-in. diameter plates, and no strains were recorded under the 8-in. plate. The position of this gauge (tangentially 3 in. from the center of the load) was comparable to that of gauge 4-1 in the case of a central loading (6 in. from the load). Relatively good agreement was found to exist between strains recorded in the two cases. When tests were made at position B, higher compressive strains were recorded. Because this strain was measured in a direction parallel to and relatively far from the edge and tangential to the load, one may expect a relatively close agreement with the readings for the same gauge under central loading. A comparison with the data for gauge 4-3 under central loading shows excellent agreement.

Gauge 4-7 recorded compressive strains at both edge load positions. As expected, the largest strains were experienced for load position B, this being the more severe loading condition and the one where the load was the closer to the gauge. With the load 8 in. from the edge, strains 2-3 times larger than those of the central loading case were measured.

On gauge 4-11, compressive strains were recorded at load position A. For load position B, strain recordings were only obtained for the 18-in. diameter plate. Although these strains were smaller than those recorded by the same gauge with the load at position A, they were slightly larger than those recorded by the gauge in the same position relative to a central load, which is to be expected. Furthermore, for load position B, the strains recorded on gauges 4-11 and 4-3 were about equal, which is reasonable according to the geometry shown in Figure 1.

METHOD OF ANALYSIS

Explicit solutions for 2- and 3-layered pavement systems and computer solutions based on multiple-layer theory and on finite-element systems are readily available for the theoretical analysis of axisymmetric (central) loading of pavements. Although these solutions are not directly applicable to the analysis of loading near a pavement edge or a crack, recent developments in finite-element analysis make it possible to also treat these cases of loading analytically.

Wilson (7) developed a finite-element computer program for a 3-dimensional prismatic solid. This program, which was adapted for pavements by Pretorius (5), was used in the present study to evaluate the effects of traffic loads close to the pavement edge. A transverse section of the structure illustrating the configuration of the finite elements (each element representing a longitudinal prism) is shown in Figure 11. Although the element properties could be varied at will in the transverse plane (limited, however, to 12 linearly elastic material types), these properties remain constant along the prisms in the longitudinal direction.

The system is essentially 2-dimensional, with the third dimension introduced into the idealized structure by expressing the load as a Fourier series in this direction. Stresses and deformations caused by each Fourier term are summed, and the process is continued until further additions become insignificant. The number of Fourier terms required increases with the ratio between the "longitudinal distance between planes of symmetry" (where the loads are applied) and the "loaded length." For a stiff pavement,

Figure 10. Resilient strains in asphalt concrete under repeated loading on edge of pavement with 5-in. asphalt concrete surfacing (load and gauge positions as shown in Fig. 1).

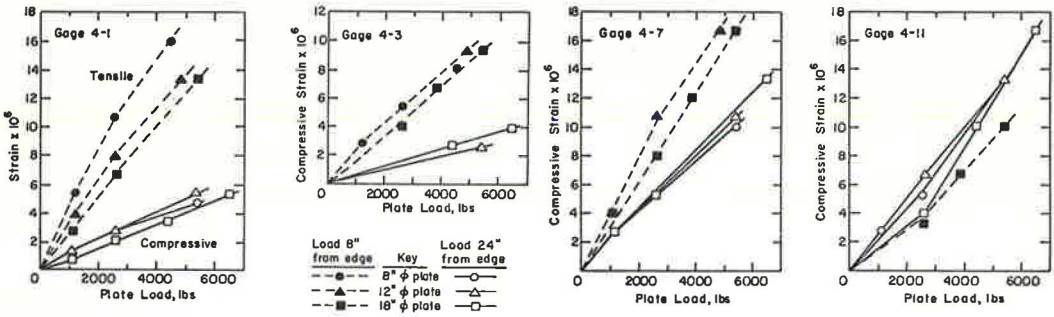

Figure 11. Finite-element mesh used for edge-loading conditions.

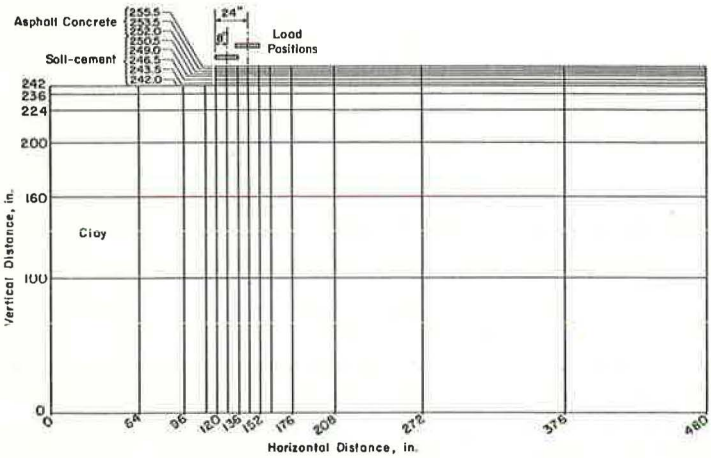

Figure 12. Finite-element mesh in vicinity of crack for plane-symmetric loading.

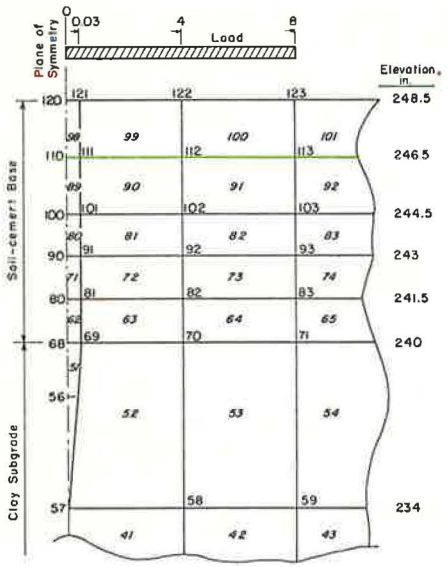

the distance between loads has to be large to avoid mutual interference, yet the loaded length has to be commensurate with the size of the loading plates. In the present study, the distance between planes of symmetry was chosen to be 240 in., and the plate size was 16 by 16 in. (corresponding to an 18-in. diameter circular plate). For these conditions 16 Fourier terms were required to obtain the desired accuracy. For the finite-element grid shown, each Fourier term required nearly 2 minutes of time on a CDC 6400 computer; hence, the complete solution took approximately half an hour. For this reason, only 2 solutions were obtained, viz., with the load center 8 in. and 24 in. from the pavement edge.

The same computer program was used to analyze stresses and deformations in the cracked soil-cement pavement. The configuration of elements used near the cracked zone is shown in Figure 12. It was assumed that the crack passed through the centerline of the loaded area. In this way, the plane of the crack acted as a plane of symmetry, and only the system on one side of the crack needed to be analyzed. This represents a less severe condition than if the total load were concentrated on one side of the crack. However, when one considers that shear stresses can be transmitted through the cracked zone, and also the likely position of the crack as shown in Figure 1, the assumed system appeared reasonable.

The finite-element grid shown in Figure 12 extends to the same depth as the grid shown in Figure 11. In the horizontal direction the subgrade extends to 240 in. and the soil-cement base extends to 120 in. from the crack, thus simulating the actual dimensions of the pavement prototype. The analysis was based on loading a 16-in. square plate and a distance between planes of symmetry of 240 in. in the longitudinal direction.

The field observations indicated that the crack caused by overloading the plate did not extend to the surface of the base. This would be expected because, even for the cracked base, the uppermost part will be subjected to horizontal compressive bending stresses. One may rationalize, therefore, that, once the base cracks in flexural tension (i.e., when the tensile stress reaches the tensile strength), the crack will propagate upward to the point where the tensile stress falls below the tensile strength. The extent of the crack propagation can be determined by analyzing the stress conditions for various crack depths. In the finite-element grid shown in Figure 12 provision was made for this procedure in that a narrow column of elements adjacent to the crack could be assigned various elastic properties. For the uncracked pavement, the narrow elements were assigned the same elastic properties as the adjacent elements. Then, assuming a crack propagating upward, we consecutively assigned elements 62, 71, 80, and 89 a very low elastic modulus (1 psi) to reflect the cracked condition.

RESULTS OF PAVEMENT ANALYSES

Cracking of Soil-Cement Base

Analyses were based on the assumption that cracks extended upward from the bottom of the soil-cement 0, 1½, 3, 4½, and 6½ in. The assumed loading was 6,400 lb on a 16-in. square plate (corresponding to an 18-in. diameter circular plate). The results of these analyses are shown in Figure 13a. In the uncracked condition the maximum tensile stress is approximately 100 psi. If a crack is initiated at this stress (i.e., if the tensile strength is 100 psi), stress concentration at the end of the crack will cause the crack to propagate. Thus, for upward crack propagations of 1½ and 3 in. the maximum tensile stress will be at least 120 psi and 140 psi respectively as shown in Figure 13a. Once the crack rises to 4½ in., a reduction of the maximum tensile stress (at the end of the crack) is evident, although it is still likely to be well above 100 psi. However, had a crack risen 6½ in. above the bottom of the slab, the computer solution indicates that only compressive stresses would occur. This may not be quite so, however, because the compressive stress indicated (40 psi) is an average of the stresses over the uncracked top 2 in. of the slab (element 98, Fig. 12). Thus, because the maximum horizontal compressive stress at the top of the element is likely to exceed 80 psi, it is likely that tensile stresses will still occur at the bottom of the element. This tensile stress is not likely to reach 100 psi, so one may assume that at

least the upper 2 in. of the pavement would remain uncracked. It should be borne in mind, however, that, because of the characteristic stress singularity at the crack tip, the finite-element solution may not be valid in this region. Hence, the stresses computed for the crack tip may be in error. A general conclusion of this analysis is, nevertheless, that, for materials and geometric conditions similar to those in this experiment, a crack in a soil-cement slab once initiated in bending is likely to extend upward some ⅔ to ¾ of the slab thickness. Such cracks once initiated in bending may ultimately extend over the full depth because of thermal and shrinkage stresses inasmuch as shrinkage and thermal cracks originate at the top surface and propagate downward.

Figure 13b shows the horizontal stresses 6 in. from the crack. As expected, a stress relaxation develops, particularly in the lower part of the slab with upward propagation of the crack. Thus, for a 6½-in. crack height, the maximum stresses at top and bottom are approximately ⅔ and ⅓ respectively of the stresses in the uncracked slab. It is noteworthy that the neutral axis stays close to the middle of the slab, even for the cracked pavement.

Figure 14a shows the crack openings calculated for various hypothetical crack depths. For a crack depth of ⅔ to ¾ of the slab thickness, a maximum crack opening of about 7 to 8 × 10^{-4} in. can be expected under the given load of 6,400 lb on a 16-in. square plate. Comparing the calculated crack opening with the field strain gauge observation (in terms of linear displacement of end platens in the LVDT type of strain gauge), we note that the field value is less than predicted. One reason for the discrepancy may be that the crack does not ideally "intersect" the gauge as assumed for the computation. The same kind of discrepancy was noted by George (4), who attributed it to viscous effects in soil-cement.

Figure 14b shows the horizontal strains in the soil-cement slab above the cracked zone for various crack depths. This diagram is in agreement with the one shown in Figure 13 for the horizontal stresses and confirms that for a crack depth of 6½ in. a slight tension will occur at the bottom of the upper 2-in. element. Good agreement is observed between the calculated strains and the field data.

Figure 15 shows vertical stresses at a 3-in. depth into the subgrade in a plane perpendicular to the plane of the crack (Fig. 15a) and in a plane parallel to and 6 in. away from the crack (Fig. 15b). Figure 15a shows that a 4½-in. crack will increase the maximum vertical stress by about 30 percent above the uncracked condition and a 6½-in. crack will increase it by about 50 percent. The latter percentage corresponds to the figure calculated on the basis of field data. Stresses observed on gauge 2-2 for loading on 12- and 16-in. diameter plates are shown in Figure 15a at about the position the gauge would have according to the crack position shown in Figure 1. We note that, although the stress recorded on gauge 2-2 for loading on a 16-in. diameter plate is less than that predicted for the cracked slab, the recorded stress for the 12-in. diameter plate is close to the predicted value.

For a plane 6 in. away from the crack, Figure 15b shows less variation in stress with crack depth than does Figure 15a for positions close to the load. Stresses observed on gauge 2-1 are shown in Figure 15b, again at about the position the gauge would have according to the position shown in Figure 1. The agreement is reasonable if the speculative nature of the positioning of the crack in relation to the gauge is considered.

Figure 16 shows the deflection patterns for the slab with cracks of different depths. The curves show relatively good agreement with the subgrade stress patterns shown in Figure 15a. From data shown in Figure 16 we can deduce that a 6½-in. crack increases the vertical deflection about 20 percent above that for the uncracked slab. This again is supported by the field observations.

Edge Loading

At both edge-loading positions A and B, 8-, 12-, and 18-in. diameter plates were used. For the computer solutions for the 2 test positions, however, only 1 plate size, 16 in. square (or 18-in. diameter), was analyzed because of the large amount of computer time required to solve the edge-loading problem.

Figure 13. Finite-element solutions for horizontal stresses in plane of tension crack and 6 in. away as functions of level of cracking of 8½-in. thick soil cement slab under 6,400-lb load on 16- by 16-in. square plate.

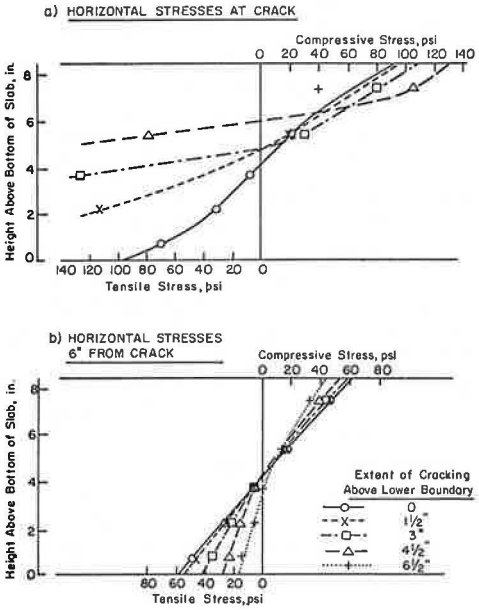

Figure 14. Finite-element solutions for crack opening and horizontal strains in uncracked portion as functions of extent of cracking of 8½-in. thick soil-cement slab under 6,400-lb load on 16- by 16-in. square plate.

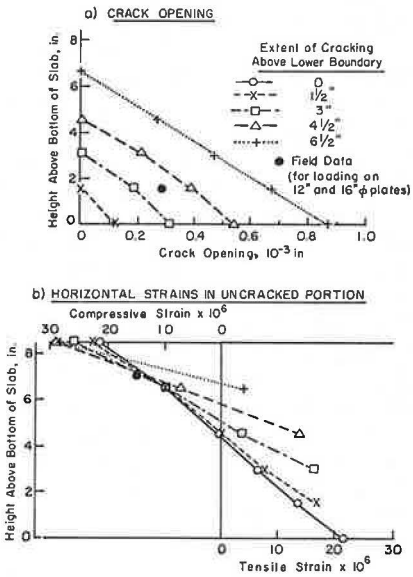

Figure 15. Finite-element solutions for vertical stresses at 3-in. depth in subgrade under cracked soil-cement slab and under 6,400-lb load on a 16- by 16-in. square plate.

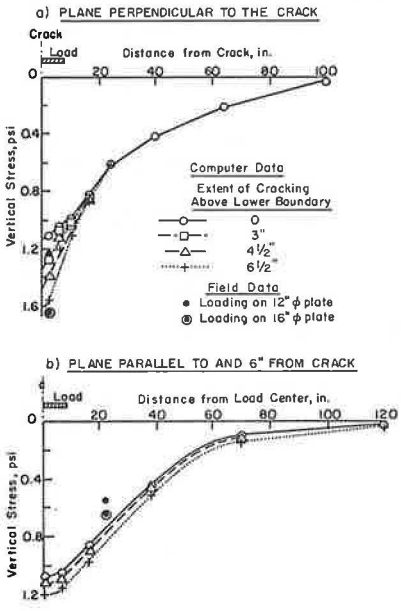

Figure 16. Finite-element solutions for deflections at various distances from tension crack in 8½-in. thick soil-cement slab as functions of extent of cracking above lower boundary under 6,400-lb load on a 16- by 16-in. square plate.

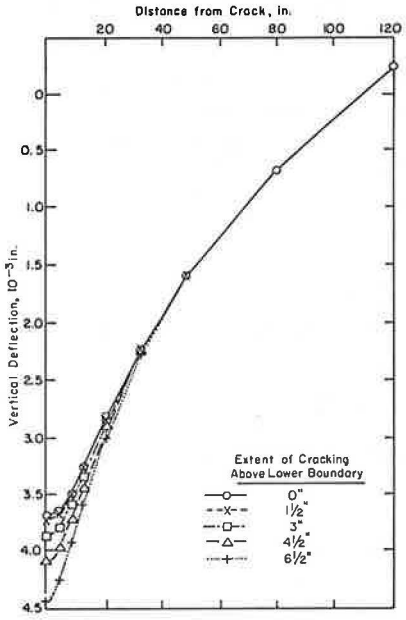

Figure 17 shows a comparison of field data and computed predictions for vertical deflections of the pavement under edge loading. Loading 24 in. and 8 in. from the edge gave computed deflections approximately 10 and 80 percent respectively above those computed for the central loading case. These percentages are somewhat higher than the corresponding field observations. The relative magnitudes of the edge-loading deflections, with the value being about 70 percent larger at position B than at position A, represent a ratio somewhat larger than that for the field data. The predictions underestimate the actual plate deflections by approximately 15 percent.

Figure 18 shows the deflection patterns with horizontal and vertical distance from the pavement edge for loading positions A and B respectively. The agreement between observed and calculated deflections is very good. Vertical stresses were recorded at 2 isolated points: at mid-depth in the base and at 6-in. depth within the subgrade. The results of the computer predictions, not reproduced here, show a satisfactory agreement between measured and predicted values for both loading positions A and B.

Figure 19 compares observed and predicted horizontal strains in the surfacing and base in a plane perpendicular to the pavement edge for loading position B. The upper diagram shows strains in the plane of the drawing, and the lower diagram shows strains in a direction perpendicular to that plane, i. e., in a plane parallel to the pavement edge. The strains are plotted along a vertical line 21 in. in from the edge of the pavement. A good agreement exists between recorded and predicted strains in the plane perpendicular to the edge (Fig. 19a). In the direction parallel to the edge (Fig. 19b), however, predicted strains are considerably larger than the recorded.

Figure 20 shows strains along a plane parallel to and 8 in. from the pavement edge for load position B (also 8 in. from the edge). The upper diagram shows horizontal strains in this plane, and the lower diagram shows the strains in a direction perpendicular to that plane. A fairly good agreement exists between the observed and the predicted values.

The following 2 important considerations from data shown in Figures 19 and 20 are applicable both to the edge-loading case and to the situation in a cracked pavement with a load approaching the crack:

1. Figure 20a confirms that for load position B critical tensile strains occur at the bottom of the soil-cement slab near the crack in the direction parallel to the crack. For the edge-loading case, which is also closely applicable for a wide shrinkage crack with little or no load transfer across the crack, this strain is some 40 to 50 percent higher than that observed in the uncracked slab (full line, Fig. 14b). Also, for the case of a "closed" crack the field experiment indicated an increase in these critical strains of about 20 percent above those for the uncracked slab (Fig. 3b). In both cases, therefore, there is a real danger that further cracking will propagate in the direction perpendicular to the existing crack; this in turn will lead to corner-loading situations in the areas adjacent to the cracks, causing further serious tensile stress conditions at the top of the base and surfacing.

2. The computer solutions confirm the recording on gauge 4-1 (Fig. 10) that, as the load approaches the crack, there is a reversal of the horizontal strains in the direction perpendicular to the crack (x-direction) in the top of the base and surfacing from compressive for load position A (not shown) to tensile for load position B (Fig. 19a). Reversal of strains from tensile to compressive also occurs at the bottom of the soil-cement slab as the load approaches the crack. As far as the soil-cement base is concerned, none of these strains is as severe as those referred to in the preceding paragraph. However, they increase in significance when the fatigue aspects of stress reversals is considered.

The two strain situations described form a sufficient rationale for formation of the well-known "ladder" cracking in the wheelpaths of pavements with cement-stabilized bases. An excellent treatise on this subject has been given by Pretorius (6).

CONCLUSIONS

The present study has demonstrated a good agreement between field observations and theoretically determined stresses and deformations associated with cracking and

Figure 17. Predicted and observed deflections at top of base for loading 8 and 24 in. from pavement edge.

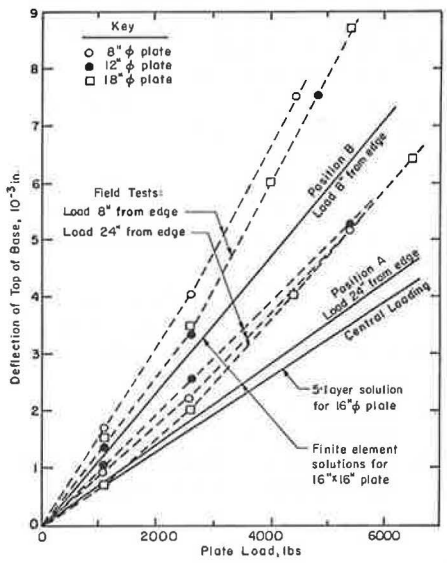

Figure 18. Vertical deflection patterns for 6,400-lb edge load on 16-in. square plate.

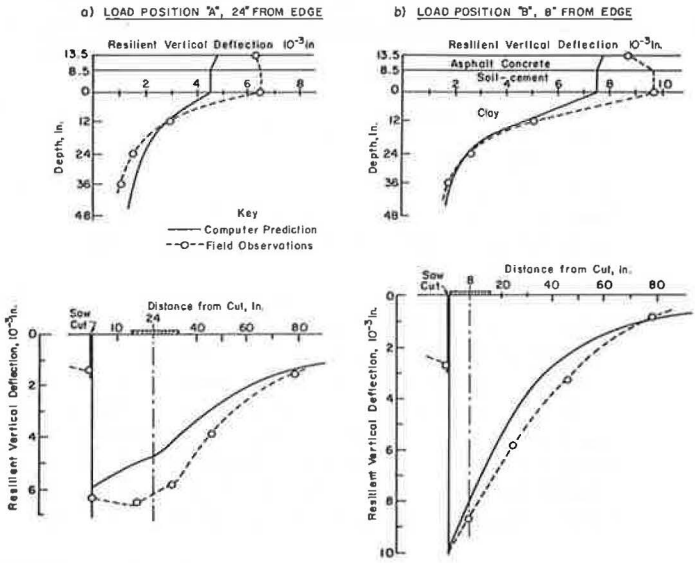

Figure 19. Horizontal strains in plane perpendicular to pavement edge under 6,400-lb loading on 16-in. square plate 8 in. from pavement edge.

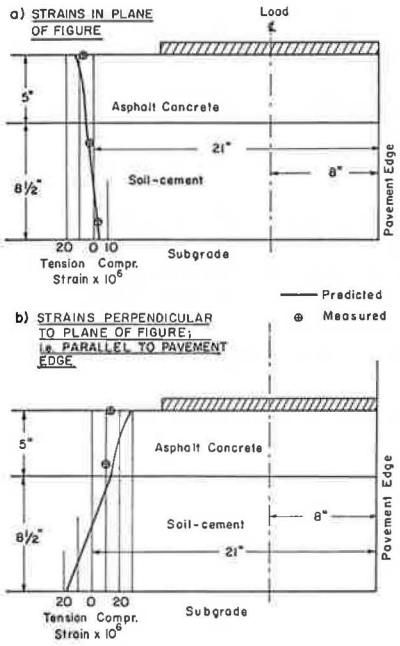

Figure 20. Horizontal strains in plane parallel to and 8 in. from pavement edge under 6,400-lb load on 16-in. square plate 8 in. from pavement edge.

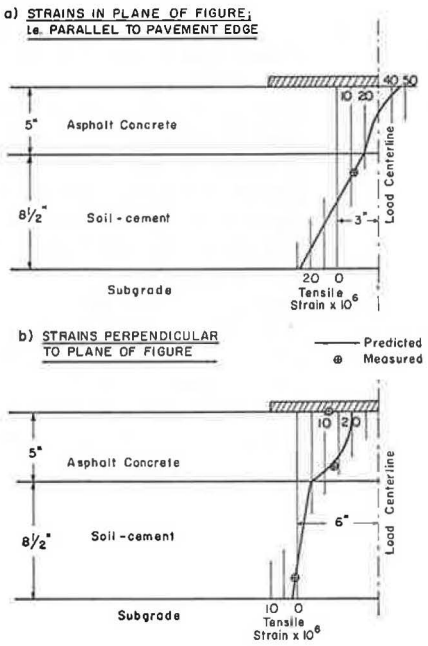

edge loading of a soil-cement pavement. The following specific conclusions can be drawn:

1. Cracking of a soil-cement pavement under loading only slightly increased (about 20 percent) vertical deflections but substantially increased (about 50 percent) vertical stresses in the subgrade near the crack when the load was placed directly over the crack. Cracking had a large influence on horizontal deformations near the crack. These data suggest that, within the reasonable range of experimental error, deflection measurements cannot be used to detect cracking of a soil-cement pavement.
2. The investigations on edge loading showed that, for the pavement structure tested in this study, loading at least 2 ft from the pavement edge can be analyzed as "central loading." Loading close to the edge is more severe in terms of stresses and deformations in both base and subgrade, however; and this should be taken account of in the pavement design.
3. Traffic loading of a soil-cement pavement where initial cracking has occurred (because of shrinkage or traffic and temperature stresses or all of these) causes critical tensile stresses and stress reversals that can explain the formation of the typical "ladder" cracking in the wheelpaths of such pavements.
4. The stiffness of an asphalt-bound layer placed on top of a layer of soil-cement has an influence on the stresses in the soil-cement layer and the deflection of the pavement structure. In this investigation 5 in. of asphalt concrete whose stiffness under the conditions of test was only about 12 percent of the soil-cement exerted a comparatively small influence on the response of the structure to load.

ACKNOWLEDGMENTS

The investigations described in this paper were made possible through a grant from the Portland Cement Association. The authors are pleased to acknowledge both this support and the helpful discussions and encouragement provided by B. E. Colley and Peter J. Nussbaum of that organization.

REFERENCES

1. Fossberg, P. E. Load-Deformation Characteristics of Three-Layer Pavements Containing Cement-Stabilized Base. Univ. of California, Berkeley, PhD dissertation, 1970.
2. George, K. P. Shrinkage Characteristics of Soil-Cement Mixtures. Highway Research Record 255, 1968, pp. 42-58.
3. George, K. P. Cracking in Cement-Treated Bases and Means for Minimizing It. Highway Research Record 255, 1968, pp. 59-71.
4. George, K. P. Cracking in Pavements Influenced by Viscoelastic Properties of Soil-Cement. Highway Research Record 263, 1969, pp. 47-59.
5. Pretorius, P. C. The Application of the Finite Element Method of Analysis to the Design of Pavements. Department of Civil Eng., Univ. of California, Berkeley, Res. Rept. CE 299, 1968.
6. Pretorius, P. C. Design Considerations for Pavements Containing Soil-Cement Base. Univ. of California, Berkeley, PhD dissertation, 1970.
7. Wilson, E. L. Analysis of Prismatic Solids. Department of Civil Eng., Univ. of California, Berkeley, unpublished, 1967.

DYNAMIC PROPERTIES OF CEMENT-TREATED SOILS

Yung-Chieh Chiang and Yong S. Chae,
Department of Civil and Environmental Engineering,
Rutgers, The State University of New Jersey, New Brunswick

An experimental study of the dynamic properties of cement-treated soils is described. The dynamic shear modulus and damping characteristics of 2 soils, a uniform sand and a silty clay, treated with Type 1 portland cement are determined by the resonant column technique. Test variables studied are cement content, confining pressure, shear-strain amplitude, and moisture content. The dynamic shear modulus and damping of both uniform sand and silty clay can be greatly increased by adding a small amount of cement. The effect of confining pressure, which increases shear modulus and damping, is more pronounced in cement-treated cohesionless soils than in cohesive soils. Higher shear-strain amplitude reduces the dynamic shear modulus and increases the damping; the cement-treated soils are subjected to a higher rate of change than are the untreated soils. The moisture content of soils has a significant effect on the dynamic properties of cement-treated cohesive soils but has no appreciable influence on cement-treated cohesionless soils. This investigation shows that the use of cement to stabilize sand and clay subjected to dynamic loading is very effective in increasing the rigidity of the soils and in reducing the deformation.

•A PROPERLY designed highway or airport pavement must meet the general requirements for all foundations. The loads imposed by traffic have to be transferred to soil layers capable of supporting them without failing in shear (bearing capacity), and the deformations of the soil layers should be such that the pavement should not suffer excessive permanent settlement. In the design and analysis of pavement-soil systems, therefore, the most critical quantities considered are the bearing capacity and deformation characteristics of the underlying soil, and those are, in turn, dependent on the material constants of the soil (such as modulus of elasticity, shear modulus, Poisson's ratio, and coefficient of subgrade reaction). The success with which the road or runway is built then depends on the accuracy with which the material properties of soil are determined.

To date, roads and runways are largely designed on the basis of knowledge of the performance of other roads built under similar traffic and subgrade conditions and of soil tests under static loading such as unconfined compression, plate loading, density, and CBR essentially dynamic nature. The use of static loading, however, does not represent the actual loading due to traffic. Because the applied load is alternating and repetitive in nature, the material properties under such a load must be investigated in terms of dynamic response and behavior of pavement-soil systems. Such a dynamic testing, in a reversed process, will also provide a rapid, nondestructive testing technique for assessing the performance of a road.

The past research indicates that theoretical values of the stresses and deformations generated by moving vehicles in multilayered elastic systems depend on the relative values of the dynamic elasticity of the layers forming the road and their thicknesses. It is, therefore, essential to obtain information concerning the dynamic material properties of the common road-making materials under repeated loading of the form applied by traffic.

For soils possessing low strength and high deformation characteristics, chemical stabilization techniques have been successfully employed in the past for road and runway construction. Studies of these stabilized soils under static loading have been extensive.

However, very little is known about the response and behavior of these soils subjected to dynamic loading.

This paper describes the first part of a two-part experimental investigation conducted to determine the dynamic properties of 2 chemically stabilized soils: a sand and a silty clay treated with cement. In the second part the 2 soils are stabilized with lime-fly ash. The experimental results on the second part will be reported in a later publication.

DETERMINATION OF DYNAMIC PROPERTIES OF SOILS

There are a number of experimental methods to determine the dynamic properties of soils. These methods may be divided into 2 general categories: (a) those in which tests are performed on a small specimen of soil usually in a triaxial compression in the laboratory (resonant column method, amplitude ratio method, and repeated-loading method) and (b) those in which the testing on soils is considered to be in situ (seismic or pulse method and elastic half-space method). A detailed discussion of these various methods (except for repeated-loading test) and a comparison of the test results obtained thereby were given by Chae (2) and will not be repeated here. A detailed description of repeated-loading technique was given by Seed and Fead (18).

Of these methods, the resonant column method has been most widely used by many researchers since Iida's original work (14) on wave propagation in sand columns. Most of these studies, however, have been confined to evaluation of cohesionless soils (4, 5, 6, 7, 11, 14, 15, 17). Few studies have been made on the dynamic behavior of clays (9, 12, 13, 20). It is believed that no work has ever been reported on chemically stabilized soils except those under repeated loading. A comprehensive test program and results were published by Mitchell et al. (16) using the repeated-loading technique.

For untreated soils it has generally been found that the most influential test parameters for sands are confining pressure and shear-strain amplitude, especially in small amplitude vibrations. Study of cohesive soils is much more complicated because of the additional variables involved, such as consolidation and other secondary effects. Specifically, a functional equation, proposed by Hardin and Black (9), for the dynamic shear modulus includes the following parameters: isotropic component of ambient effective stress, void ratio, ambient stress and vibration history, degree of saturation, deviatoric ambient stress, grain characteristics, amplitude of vibration, secondary effects that are functions of time and load increment, soil structure, and temperature.

For chemically stabilized soils the additional major parameters are cement or chemical agent content and moisture content.

EXPERIMENTAL INVESTIGATION

Materials

The materials used for this study were a uniform sand and a fine silty clay. These 2 soils were mechanically separated from the same parent material, a glacial outwash locally known as Dunellen soil, so that a comparison could be made of the dynamic response of coarse-grained soil and fine-grained soil from the same parent material. The grain size distribution curves for both soils are shown in Figure 1. The sand particles ranged from 2 to 0.074 mm in diameter and had a uniformity coefficient of 3.43 and a specific gravity of 2.63. The clay had a specific gravity of 2.65, liquid limit of 30.1 percent, and plasticity index of 9.8 percent. According to AASHO classification, the sand is classified as A-3 and clay as A-6. Type 1 portland cement was used throughout the investigation.

Specimen Preparation

Tests were performed on remolded specimens prepared by a modified Harvard miniature compactor. A hammer, 0.75 in. in diameter and weighing 0.82 lb, was dropped 6 in. to compact the specimen in 5 layers with 10 drops on each layer. The size of the

specimen after extrusion was 1.31 in. in diameter and 2.93 in. in height. Based on strength criteria, cement contents for both sand and clay were chosen at 2, 4, and 6 percent of the dry weight of soil. A soil-cement mixture was dry-mixed, and a predetermined amount of distilled water was added to bring the mixture to a desired moisture content. The mixture was mixed thoroughly, and the specimen was molded immediately. The moisture-density curves for the sand and the silty clay are shown in Figure 2. With changes in cement content, for the sand the optimum moisture content does not vary significantly but does vary markedly for the silty clay.

Immediately following the extrusion, each specimen was wrapped in plastic and placed in a glass container to prevent moisture change and absorption of CO_2. The specimens were then stored in a water bath where 70 F temperature and 95 percent relative humidity were maintained at all times. The cement-treated soils were cured for 28 days before testing. The cement-treated sand specimens were first cured in the compaction mold and were extruded after 2 weeks of curing.

Test Setup and Procedure

The dynamic shear modulus and damping were determined by means of the resonant column technique in torsion. Figure 3 shows a schematic diagram of the instrumentation sequences in the overall test setup. Figure 4 shows a view of the overall setup in the laboratory. The apparatus consists essentially of a driving mechanism (oscillator) on a specimen contained in a triaxial chamber and auxiliary equipment for excitation and readout. The torsional oscillator used was developed by Hardin. A detailed description of the oscillator and the theory of vibration for the specimen-apparatus model may be found in an article by Hardin and Music (10). Torque is applied to the center ring of this mechanism by applying sinusoidally varying voltage to the coils, producing sinusoidally varying forces between the coils and magnets. For balancing the weight of the apparatus on the specimen, a loading truss and lever-fulcrum are used outside the cell. Because the specimen is fixed at the bottom, a free-fixed end condition results in the vibration.

After the equipment was connected as shown in Figures 3 and 4 the input current was set at a desired level and kept constant. The frequency was varied over a large range to find the approximate position of the resonant frequency. When the approximate position had been ascertained, the frequency was varied in much smaller increments for precise measurement of the resonant frequency. The peak-to-peak value of acceleration and the phase angle between the input force and acceleration were recorded at each frequency. The dynamic response data so obtained, together with the apparatus-specimen parameters, were fed into a computer based on the theory of the apparatus-specimen model developed by Hardin (10). The dynamic shear modulus was determined by the process of iteration. Damping characteristics in terms of logarithmic decrement were obtained from the frequency-displacement amplitude response curves.

The independent test variables were moisture contents and cement contents for the specimens and confining pressures and shear-strain amplitudes for the testing apparatus. The specimens were tested at confining pressures of 3, 10, 20, and 35 psi. At a given confining pressure application, the dynamic shear modulus and damping were determined in sequence at the following 5 preselected shear-strain amplitudes: 1.4×10^{-5}, 2.3×10^{-5}, 3.7×10^{-5}, 7.5×10^{-5}, and 1.4×10^{-4}. The strain amplitudes used were limited to these values because of restrictions imposed by the apparatus and the specimen. These strain amplitudes may be small for traffic loading on real pavements, except perhaps that in the underlying subgrade layer; nevertheless, the test results obtained will be useful for they may be correlated with those expected in a real situation.

Immediately after the resonant column test, the specimens were tested in a triaxial apparatus for the evaluation of static properties of the soils. The confining pressure was chosen at 20 psi and the strain rate at 0.02 in./min. The stress-strain relationship for each specimen was then plotted by computer.

Figure 1. Grain size distribution.

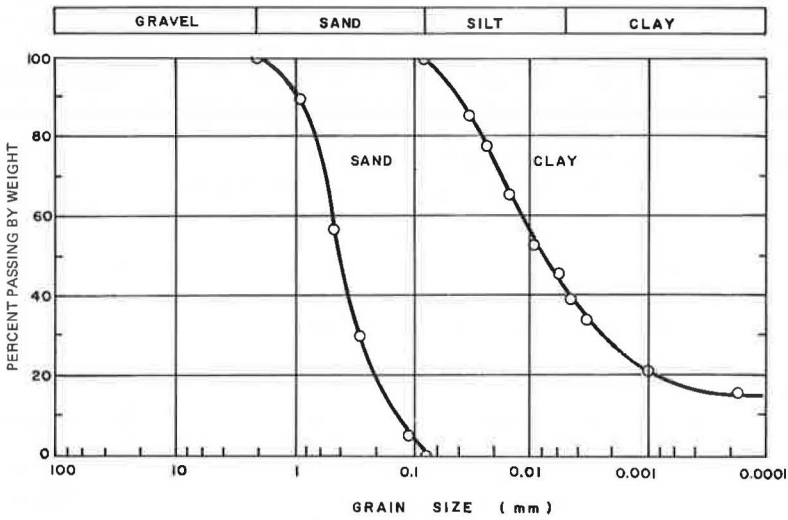

Figure 2. Density versus moisture content for sand and clay.

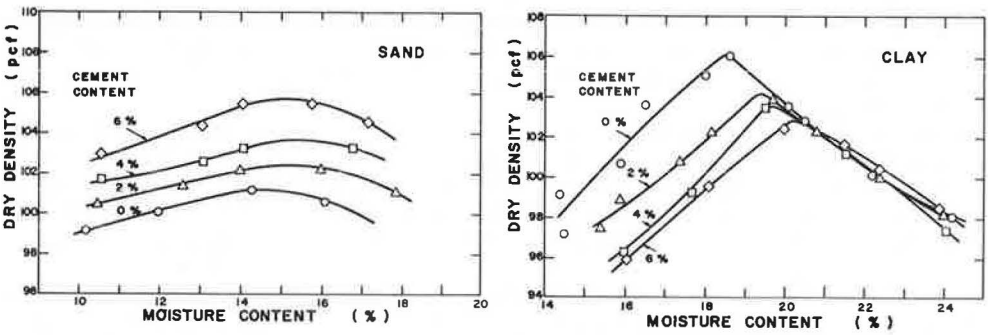

Figure 3. Schematic of overall test setup.

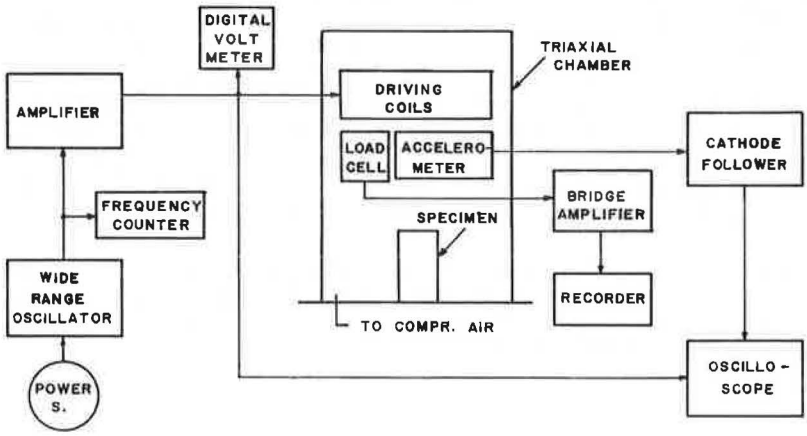

ANALYSIS OF TEST RESULTS

Many variables are involved in a single test, and their interrelations must be considered in the analysis of test results. The variables may include confining pressure, shear-strain amplitude, cement content, moisture content, density, void ratio, and degree of saturation. Consequently, when the effect of one variable on the dynamic properties of a material is evaluated alone, the other variables must be kept constant and the interrelations among these variables should be known.

DYNAMIC SHEAR MODULUS

Effect of Confining Pressure

Variations of dynamic shear modulus with confining pressure for sand and clay are shown in Figures 5 and 6. Each line shown in these figures represents the response of a specific specimen at the optimum moisture content. Only the results at a specific shear-strain amplitude (1.4×10^{-5}) are given. Similar results were obtained at various levels of strain amplitude. In general, dynamic shear modulus increases with increasing confining pressure and can be plotted as a straight line in a log-log scale. The increase in shear modulus with increased confining pressure becomes more pronounced for sand with greater cement content as indicated by the slope of the shear modulus-confining pressure curves. The slope increases from 0.50 for untreated sand to 0.86 for 6 percent cement-treated sand. On the other hand, the rate of increase of shear modulus for the silty clay samples remains essentially the same at 0.45 irrespective of cement content. The results obtained in this study indicating that dynamic shear modulus for both untreated sand and clay varies with approximately 0.5 power of confining pressure confirm the previous test results obtained by many investigators (4, 5, 7, 9, 12, 13). An empirical equation for the dynamic shear modulus of dry sand was proposed by Hardin (7). For small strain amplitudes,

$$G = \{[2{,}630(2.17 - e)^2]/1 + e\}\ \bar{\sigma}^{0.5} \tag{1}$$

in which G is the dynamic shear modulus in psi, e is the void ratio, and $\bar{\sigma}$ is the effective confining pressure in psi. For the purpose of comparison, Hardin's equation using e = 0.633 is shown in Figure 5. There is a reasonably good agreement between Hardin's equation and the results obtained in this study for untreated soils. The effect of moisture appears to be negligible, as will be explained in a later section. On the basis of this agreement an effort has been made to find a general mathematical expression to accommodate cement content as a variable. The straight-line relationship of a log-log plot gives a general form of $G = a \times \sigma^b$ in which a is the unit intercept and b is the slope of the line. By obtaining the relation between cement content, a and b, one can express the modified equation as

$$G^* = (G - 0.343 \times C \times \bar{\sigma}^{0.5})\ \bar{\sigma}^{0.06C} \tag{2}$$

where G^* and G are the dynamic shear moduli in psi of cement-treated and untreated soils respectively C is the cement content in percent, and $\bar{\sigma}$ is the confining pressure in psi.

Based on the study of normally consolidated clay with low surface activity, Hardin and Black (9) also proposed a dynamic shear modulus equation for clay as follows:

$$G = \{[1{,}230\ (2.973 - e)^2]/(1 + e)\}\ \bar{\sigma}^{0.5} \tag{3}$$

This equation (with e = 0.561) is shown in Figure 6. By the same procedure, the modified dynamic shear modulus equation is determined for cement-treated clays as follows:

Figure 4. Test setup equipment.

Figure 5. Variation of dynamic shear modulus with confining pressure and cement content for sand.

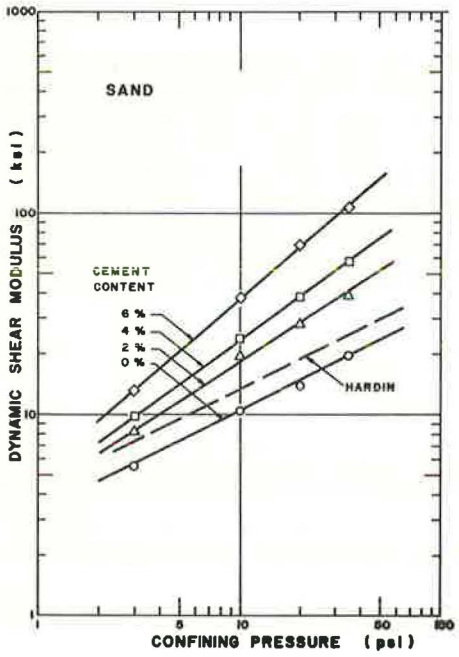

Figure 6. Variation of dynamic shear modulus with confining pressure and cement content for clay.

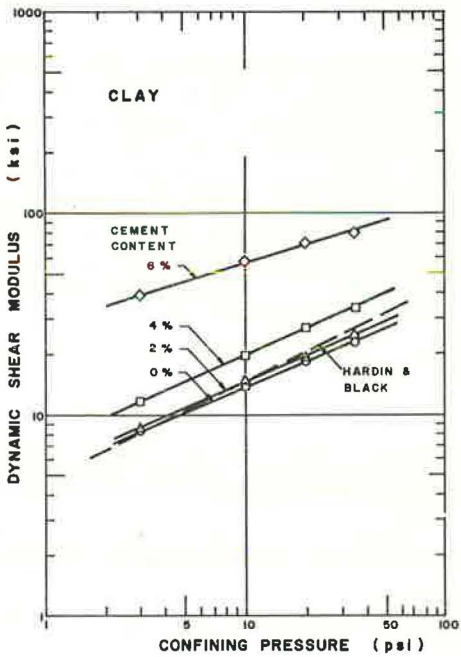

$$G^* = G + C\,[1{,}269 - 2{,}784C + 1{,}826C^2 - 440C^3 + 37C^4]\,\bar{\sigma}^{0.45} \qquad (4)$$

In using these 2 modified equations, one should take care to note the comparable features such as chemical compositions, soil structure, and strain amplitude. As will be seen later on the shear modulus-strain amplitude curves, the slope for both cement-treated and untreated soils change significantly at higher amplitude.

The slope of dynamic shear modulus-confining pressure curves for sand increases with an increasing strain amplitude imposed. The same was observed for untreated soils, although to lesser degrees, by Silver and Seed (19) using a dynamic simple shear device.

Effect of Strain Amplitude

The dynamic shear modulus as a function of shear-strain amplitude for various confining pressures and cement contents is shown in Figures 7 and 8. The dynamic shear moduli of both sand and clay decrease with increasing strain amplitude, and the rate of decrease is much more pronounced with higher cement content and confining pressure.

Within the range of shear strain studied, the average decrease of dynamic shear modulus is about 55 percent for a 6 percent cement-treated sand specimen but only 25 percent for an untreated sand specimen. Relatively speaking, the effect of cement content on dynamic shear modulus within the strain amplitude studied is small for clay soils. With the largest strain imposed, the shear modulus is reduced by about 20 percent for untreated clay and 30 percent for 6 percent cement-treated clay.

The maximum values of the dynamic shear modulus for both cement-treated and untreated clays usually occur at very small shear-strain amplitude in the 0.5×10^{-5} range. Cohesionless soils, on the other hand, exhibit different behavior in that the maximum dynamic shear moduli for cement-treated sands occur near the zero-strain amplitude. This is especially true for soils at higher cement-treatment levels.

Effect of Moisture Content

Figure 9 shows that the dynamic shear modulus of sand does not vary significantly with moisture content for a given cement content and strain level. The presence of water does not appear to reduce the velocity of wave propagation significantly in either untreated or treated sands. Similar results were obtained by Barkan (1) on Young's modulus of sand with moistures ranging between 0 and 10 percent. Hardin and Richart (11) observed that the presence of moisture in sand reduced the shear modulus slightly when the moisture is less than about 1.4 percent, but higher moisture contents do not affect the value of dynamic shear modulus.

The results for shear modulus-moisture relations for cohesive soils are quite different as shown in Figure 10. For a given confining pressure and cement content, the maximum value of dynamic shear modulus occurs near the optimum moisture but drops sharply with a further increase in moisture. For clay specimens with moisture content less than the optimum the dynamic shear modulus remains close to its maximum value. This is true for both cement-treated and untreated clay specimens within the moisture range studied and regardless of the shear-strain amplitude level. A similar observation was noted by Barkan (1) on Young's modulus of clay samples with moisture ranging from 0 to 30 percent. In studying compacted kaolinite at low stresses, deGraft-Johnson (3) also found similar results.

Effect of Cement Content

The effects of cement content have been discussed along with the other parameters in previous sections. Figures 11 and 12 show the relation between the shear modulus and cement content at the given strain amplitude of 1.4×10^{-5} and optimum moisture conditions. Cement content strongly influences the shear modulus for both sand and clay. On a semilog plot, a straight line is obtained for sand over the range of cement content tested. For clay, however, the rate of increase becomes greater as the cement content is increased. Cement stabilization can be used very effectively in weak soils

Figure 7. Variation of dynamic shear modulus with shear-strain amplitude for sand.

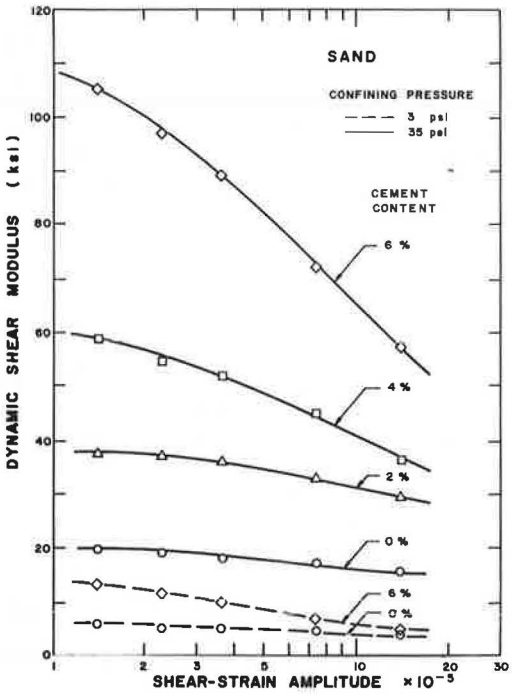

Figure 8. Variation of dynamic shear modulus with shear-strain amplitude for clay.

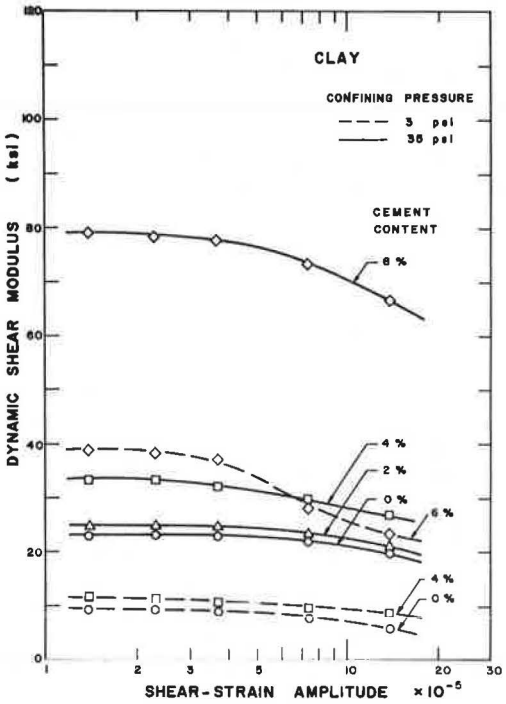

Figure 9. Variation of dynamic shear modulus with moisture content for sand.

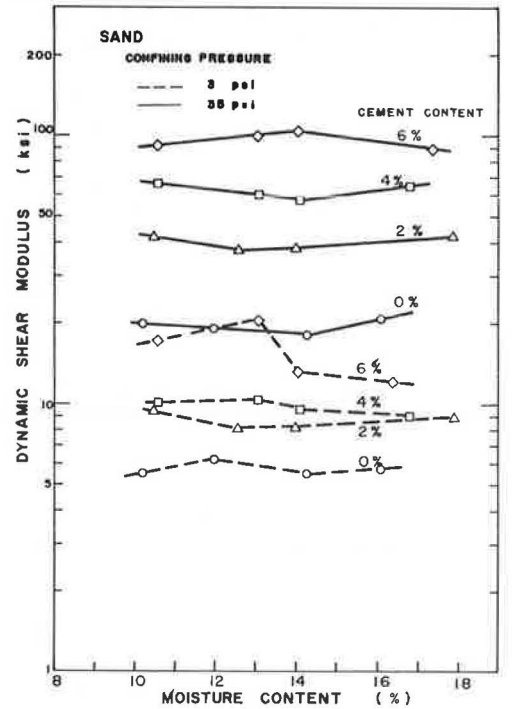

Figure 10. Variation of dynamic shear modulus with moisture content for clay.

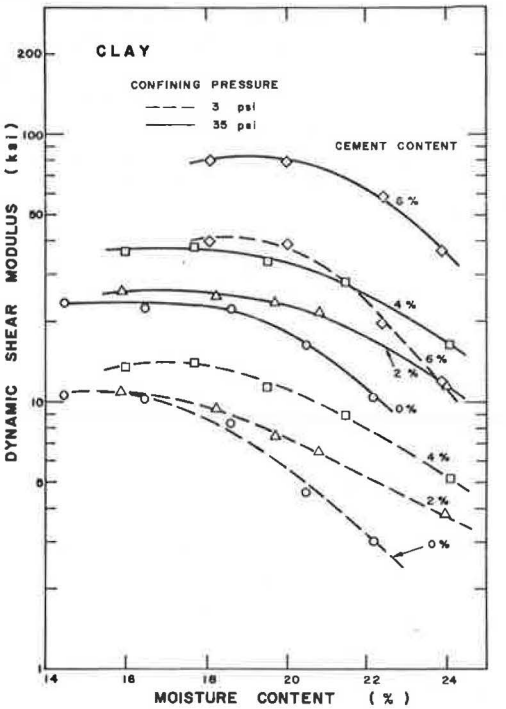

Figure 11. Effect of cement content on the dynamic shear modulus of sand.

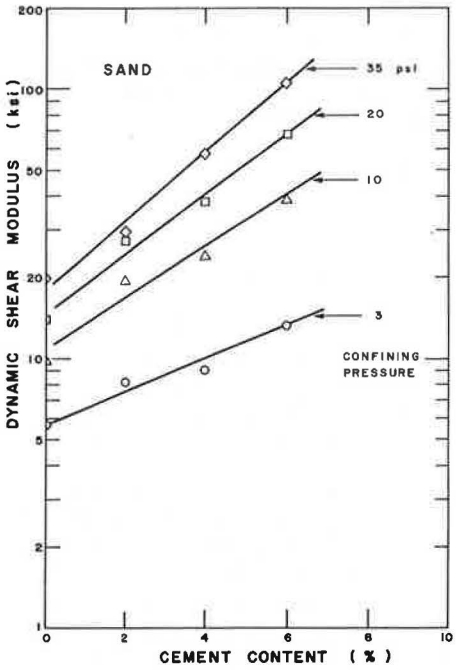

Figure 12. Effect of cement content on the dynamic shear modulus of clay.

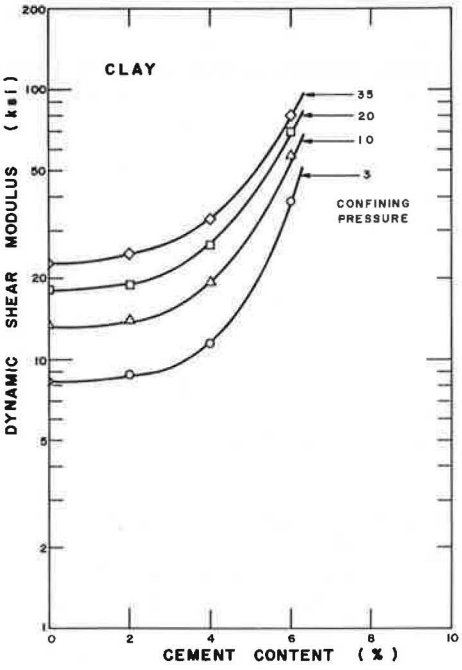

Table 1. Effect of cement content on static and dynamic properties.

Soil	Cement Content (percent)	Static Modulus of Elasticity (psi)	Dynamic Shear Modulus (psi)	Logarithmic Decrement
Sand	0	645	13,684	0.1264
	2	2,050	27,441	0.3174
	4	2,360	38,456	0.5369
	6	6,870	67,856	0.7192
Clay	0	790	18,114	0.2210
	2	800	18,700	0.2220
	4	2,130	26,633	0.2422
	6	8,600	70,447	0.3812

Note: Confining pressure = 20 psi.

Figure 13. Variation of logarithmic decrement with confining pressure and cement content for sand.

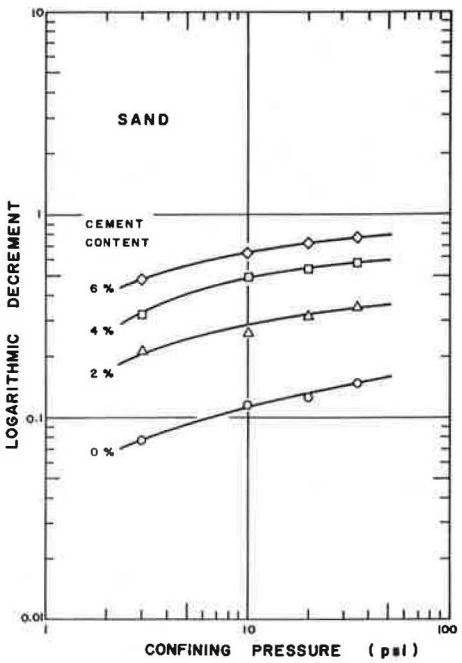

because of increased rigidity of soils subjected to dynamic loading. Table 1 gives typical results obtained for static and dynamic properties of the sand and silty clay tested under the same confining pressure of 20 psi. The static modulus of elasticity was taken to be secant modulus at one-third of the ultimate load. Both the static and dynamic moduli increase with an increasing cement content as expected. However, because of the many test parameters involved in both static and dynamic tests, quantitative correlations between dynamic and static response are difficult.

DAMPING CHARACTERISTICS

Effect of Confining Pressure

The test results for logarithmic decrement and confining pressure relations for sand specimens treated at different cement contents are shown in Figure 13 for small strain amplitude of 1.4×10^{-5}. In general, damping increases with confining pressure, and the greatest increase occurs at low confining pressures. The curves are mostly parallel to each other, indicating that the rate of change in damping for sand specimens is independent of cement content. For the silty clay no consistent trend was observed because of the very strong influence of moisture content on damping as will be explained later.

Damping characteristics of granular soils have been measured by several investigators (6, 8) using a vibrational decay technique in a resonant test. Hardin (8) showed that logarithmic decrement decreases with 0.5 power of confining pressure. Damping in clays was studied by Humphries (12), who found that logarithmic decrement of clay increased with 0.3 to 0.7 power of confining pressure. Humpries also compared the results of logarithmic decrement as determined by the amplitude-frequency method and decay method and found that when logarithmic decrement was small both methods gave the same value, but the logarithmic decrement as determined from the decay method yielded a higher value when the logarithmic decrement was large.

Effect of Shear-Strain Amplitude

Figures 14 and 15 show the relations among logarithmic decrement, strain amplitude, cement content, and confining pressure. For all soils, logarithmic decrement increases with shear-strain amplitude, and the greater increase is at larger amplitude. A greater increase in damping is also observed in soils with higher cement content and larger confining pressure as previously stated.

Effect of Moisture Content

Figure 16 shows that the damping characteristics of sand is independent of the moisture as was the case for shear modulus. Damping capacity of sand can be improved by the addition of cement regardless of its moisture condition.

The effect of moisture on damping in cohesive soils is shown in Figure 17. Under low confining pressure damping is reduced as moisture is increased, but under high confining pressure the same trend is not observed. For specimens having moisture content higher than the optimum, an increase in confining pressure increases damping; for specimens having moisture content lower than the optimum, an increase in confining pressure decreases damping. This is true for both untreated and treated clay specimens.

Effect of Cement Content

The effect of cement content on damping has been discussed in conjunction with the effects of the other parameters previously. In general, an increase in cement content increases damping and dissipates larger wave energy as confining pressure is increased. This is an advantage in practical design of roadways because of reduction in amplitude of vibration. Table 1 gives the effect of cement content on attenuation of wave energy. At a constant confining pressure of 20 psi and a 6 percent cement-treatment level, the increase of logarithmic decrement is 5.7 times for sand and only 1.7 for clay, although the increase of static strength is much higher for clays.

Figure 14. Effect of shear-strain amplitude and cement content on logarithmic decrement of sand.

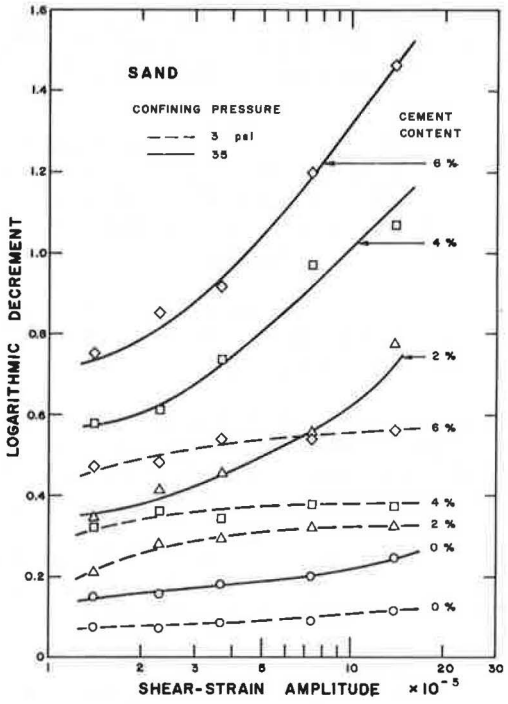

Figure 15. Effect of shear-strain amplitude and cement content on logarithmic decrement of clay.

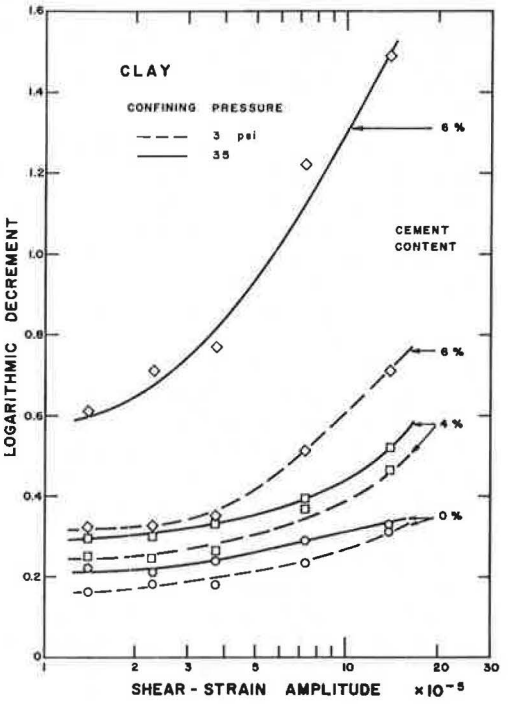

Figure 16. Variation of logarithmic decrement with moisture content for sand.

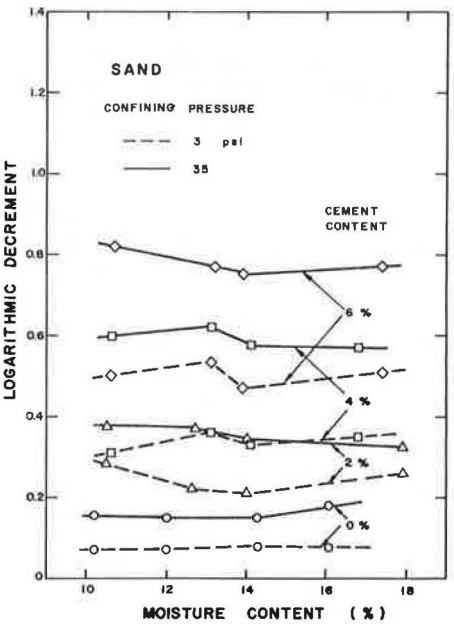

Figure 17. Variation of logarithmic decrement with moisture content for clay.

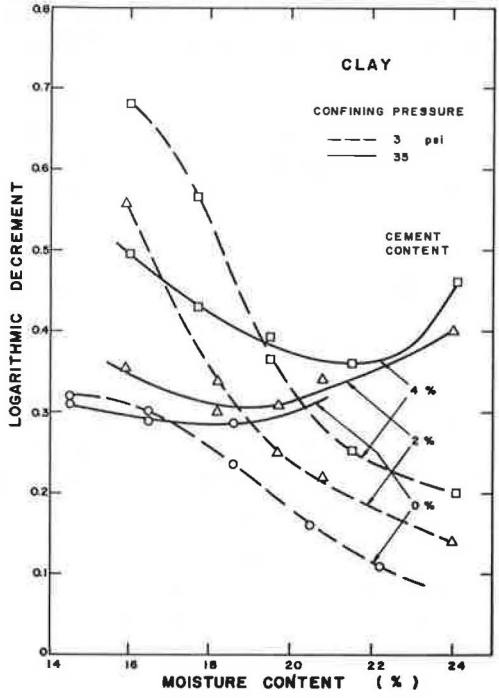

CONCLUSIONS

The use of cement to stabilize sand and clay subjected to dynamic loads is very effective in increasing the rigidity of the soil and in reducing the deformation. When resonance is a problem in foundation design, this condition may be avoided successfully by cement stabilization that produces changes in the elastic properties of the soil. The essential conclusions to be derived from this experimental study are summarized as follows:

1. Dynamic shear moduli for both sand and clay increase with increasing confining pressure. Cement treatment of both soils results in a significant increase in dynamic shear modulus, and the effect is more pronounced at a higher confining pressure for sand. Modified equations for dynamic shear moduli for cement-treated sand and clay at small shear-strain amplitudes are derived as functions of confining pressure, void ratio, and cement content.
2. Dynamic shear moduli for both materials decreased with increasing shear-strain amplitudes, and the effect is most pronounced at a small strain amplitude within the range studied. Cement-treatment increases the rates of change of the dynamic shear moduli at various strain amplitudes for both soils.
3. At a given confining pressure, cement content, and strain amplitude the dynamic shear modulus does not vary significantly with moisture for cohesionless soils. For clay soils, however, it decreases rapidly when the moisture of the specimen is increased beyond the optimum moisture content; the maximum value occurs near the dry side of the optimum.
4. Logarithmic decrement of sand does not vary with moisture content of the specimen. Higher confining pressure and cement content will result in higher damping. Logarithmic decrement in clay, both untreated and treated, depends on the relative amount of moisture with respect to the optimum.
5. Logarithmic decrement increases with increasing shear-strain amplitude for both materials. Within the range of the strain amplitude studied, damping increases at a faster rate in cement-treated clay specimens than in untreated ones. However, the rate of change remains about the same for sand.
6. The practical aspect of this study is the effect of cement treatment of soils on the increase of both dynamic shear modulus and logarithmic decrement. The combined effect of these properties can be utilized to a great advantage in designing cement-stabilized soil-foundation system subjected to dynamic loading.

ACKNOWLEDGMENTS

The authors are grateful to the Rutgers Research Council for supporting this research. Computer time was made available through the facilities of the Rutgers University Computing Center.

REFERENCES

1. Barkan, D. D. Dynamics of Bases and Foundations. McGraw-Hill, New York, 1962.
2. Chae, Y. S. The Material Constants of Soils as Determined From Dynamic Testing. Proc., Symposium on Wave Propagation and Dynamic Properties of Earth Materials, Univ. of New Mexico, Aug. 1967, pp. 759-770.
3. deGraft-Johnson, J. W. S. The Damping Capacity of Compacted Kaolinite Under Low Stresses. Proc., Symposium on Wave Propagation and Dynamic Properties of Earth Materials, Univ. of New Mexico, Aug. 1967, pp. 771-779.
4. Drnevich, V. P. Effect of Strain History on the Dynamic Properties of Sand. Univ. of Michigan, Ann Arbor, PhD thesis, 1967.
5. Drnevich, V. P., and Richart, F. E., Jr. Dynamic Prestraining of Dry Sand. Jour. Soil Mech. and Found. Div., Proc. ASCE, Vol. 96, No. SM2, March 1970, pp. 453-469.
6. Hall, J. R., and Richart, F. E., Jr. Dissipation of Elastic Wave Energy in Granular Soils. Jour. Soil Mech. and Found. Div., Proc. ASCE, Vol. 89, No. SM6, Nov. 1963, pp. 27-55.

7. Hardin, B. O. Dynamic Versus Static Shear Modulus for Dry Sand. Materials Research and Standards, ASTM, Vol. 5, No. 5, May 1965, pp. 27-42.
8. Hardin, B. O. The Nature of Damping in Sands. Jour. Soil Mech. and Found. Div., Proc. ASCE, Vol. 91, No. SM1, Jan. 1965, pp. 63-97.
9. Hardin, B. O., and Black, W. L. Vibrations Modulus of Normally Consolidate Clay. Jour. Soil Mech. and Found. Div., Proc. ASCE, Vol. 94, No. SM2, March, 1968, pp. 353-369, and Closure, Vol. 95, No. SM6, Nov. 1969, pp. 1531-1537.
10. Hardin, B. O., and Music, J. Apparatus for Vibration of Soil Specimens During the Triaxial Test. ASTM, Spec. Tech. Publ. 392, 1965, pp. 55-74.
11. Hardin, B. O., and Richart, F. E., Jr. Elastic Wave Velocities in Granular Soils. Jour. Soil Mech. and Found. Div., Proc. ASCE, Vol. 89, No. SM1, Feb. 1963, pp. 33-65.
12. Humphries, W. K. The Effect of Stress History on the Dynamic Response of Clay Soils. North Carolina State Univ., Raleigh, PhD thesis, 1966.
13. Humphries, W. K., and Wahls, H. E. Stress History Effects on Dynamic Modulus of Clay. Jour. Soil Mech. and Found. Div., Proc. ASCE, Vol. 94, No. SM2, March 1968.
14. Iida, K. The Velocity of Elastic Waves in Sand. Earthquake Research Institute Bull., Tokyo Imperial Univ., Vol. 16, 1938, pp. 131-144.
15. Iida, K. On the Elatic Properties of Soil Particularly in Relation to Its Water Content. Earthquake Research Institute Bull., Tokyo Imperial Univ., Vol. 18, 1940, pp. 675-690.
16. Mitchell, J. K., et al. Behavior of Stabilized Soils Under Repeated Loading. U. S. Army Engineer Waterways Experiment Station, Vicksburg, Miss., Corps of Engineers, Contract Rept. 3-145, 1965-1969.
17. Richart, F. E., Jr., Hall, J. R., Jr., and Lysmer, J. Study of the Propagation and Dissipation of Elastic Wave Energy in Granular Soils. Univ. of Florida, Sept. 1962.
18. Seed, H. B., and Fead, J. W. N. Apparatus for Repeated Load Tests on Soils. ASTM, Spec. Tech. Publ. 254, 1959.
19. Silver M. L., and Seed, H. B. Deformation Characteristics of Sands Under Cyclic Loading. Jour. Soil Mech. and Found. Div., Proc. ASCE, Vol. 97, No. SM8, Aug. 1971, pp. 1081-1098.
20. Wilson, S. D., and Dietrich, R. J. Effect of Consolidation Pressure on Elastic and Strength Properties of Clay. Proc., ASCE Research Conf. on Shear Strength of Cohesive Soils, Boulder, Colo., June 1960, pp. 419-435.

PERFORMANCE OF SOIL-CEMENT TEST PAVEMENT IN RHODE ISLAND

Mian-Chang Wang, Kendall Moultrop, and Vito A. Nacci,
Department of Civil Engineering, University of Rhode Island

A test road containing 2 control sections with conventional design and 5 sections with different soil-cement base and subbase was constructed in July 1967. Performance of the test road has been evaluated by using the Benkelman beam test, plate bearing test, roughometer test, crack survey, and frost study. Results obtained to date indicate that the soil-cement pavement possesses greater rigidity but develops cracks; the total length of the cracks increases with increasing curing time. An addition of 1 percent Na_2SO_4 seems to increase the rate of crack development. Cracking could result in pavement surface roughness; however, no conclusive results indicate that cracking could cause a reduction of pavement stiffness.

•AN INVESTIGATION was made of the feasibility of using stabilized local silty soils as base and subbase course materials for construction of flexible pavements in Rhode Island. A 4,130-ft test road was constructed in July 1967 for confirming and modifying the predicted conclusions of the laboratory studies (1) and for evaluating under field conditions the long-term properties of various stabilized soils.

The test road, a 2-lane highway with 10-ft shoulders, is essentially a section on RI-214, a state secondary highway in Middletown, Rhode Island. The average daily traffic (ADT) on the test road, according to a previous report (2), was 4,180; approximately 2 percent of the traffic is trucks, and 81 percent of the trucks are single-axle straight trucks. Since the road was completed, the ADT has steadily increased to 7,000 in 1970.

The test road is composed of 2 control sections of conventional design and 5 experimental sections of different materials in base and subbase courses as shown in Figure 1. All sections are surfaced with 3 in. of bituminous concrete. Moisture and temperature gauges are installed as one unit at stations 16+00, 22+00, and 26+00. The gauges are located beneath the centerline and 11 ft from the centerline on each side at depths of 6, 11, 15, 19, and 24 in. at stations 16+00 and 26+00 and at depths of 11, 15, 19 and 24 in. at station 22+00.

The soil used for construction has classifications ranging from A-2 (4) to A-4 (3) and is predominantly A-4. The index properties of a typical soil are as follows:

Property	Value
Specific gravity	2.70
Atterberg limits, percent	
Liquid limit	21
Plastic limit	NP
Textural composition, percent	
Gravel, 3 in. to 2.00 mm	20.5
Sand, 0.074 to 0.005 mm	46.0
Clay, 0.005 mm	4.0
AASHO classification	A-4(3)

Type 1 portland cement was used throughout. A trace amount (1 percent) of sodium sulfate, which was supplied in granular form, was used in sections 6 and 7 because it was concluded from previous laboratory studies (1) that an addition of 1 percent Na_2SO_4

could result in a greater strength and a considerably more rapid strength gain. Details on design and construction of the test road are given elsewhere (3, 4).

Performance of the test road and the results of laboratory tests on field and laboratory compacted samples in the first year after completion of the test road are given in other reports (2, 5). This paper presents the results of field studies obtained to date.

PERFORMANCE OF TEST PAVEMENT

The test pavements were evaluated according to their relative performance under loading and environmental influence. The performance under loading was determined by using the Benkelman beam test, plate bearing test, and roughometer test; the performance under environmental influence was evaluated on the basis of cracking and response to freezing temperature.

Benkelman Beam Test

Since the summer of 1967, Benkelman beam tests have been conducted annually in the spring and summer at the locations shown in Figure 2. The truck used for testing had a rear axle load of 18 kips and a tire pressure of 80 psi. Detailed testing procedures are given in another report (5).

Typical pavement surface deflection profiles under the test truck are shown in Figure 3. Each data point is the average of 4 measurements. There is a fairly constant deflection in both lanes, and pavement materials are rather uniformly distributed through each section. Sections 1, 2, and 4 give greater deflections and steeper slopes of profile than other sections because of the use of penetrated rock as base course material in those sections. The penetrated rock generally gives lower supporting capacity than soil-cement for the latter possesses a measurable flexural strength.

A comparison of pavement deflection measured in spring and summer is shown in Figure 4. Deflections in the spring are greater than those in the summer probably because of greater rainfall in the spring and effects of the spring thaw. According to the Newport Water Department Weather Station, the accumulated 3-day and 7-day rainfall immediately prior to Benkelman beam tests were as follows:

Test Date	7 Days (in.)	3 Days (in.)
Summer		
8-9-67	0.96	0.17
8-26-68	0.11	0
8-29-69	0.02	0.02
8-24-70	1.34	1.23
Spring		
4-18-68	0.66	0.66
4-1-69	0.49	0.38
3-23-70	1.85	1.64
4-8-71	1.60	1.05

Although moisture readings were obtained for varying depths up to 24 in., only some of the values indicate a higher moisture content in the spring. The rest of the readings varied so little or were so erratic that it was not possible to draw reliable conclusions. Higher moisture contents at greater depths might have occurred, but no field readings are available to verify this possibility.

The curve of deflection measured in the summer (Fig. 4) indicates a trend of decreasing surface deflection with increasing time and eventually approaches a constant for all sections except sections 2 and 4. For the soil-cement sections, this effect is primarily attributed to the strength increase with time (Fig. 5). Because the strength of gravel is not a function of elapsed time after compaction, the same reasoning cannot be applied to the decrease in deflection with time for control sections 1 and 4. The

Figure 1. Bases and subbases of sections of experimental road.

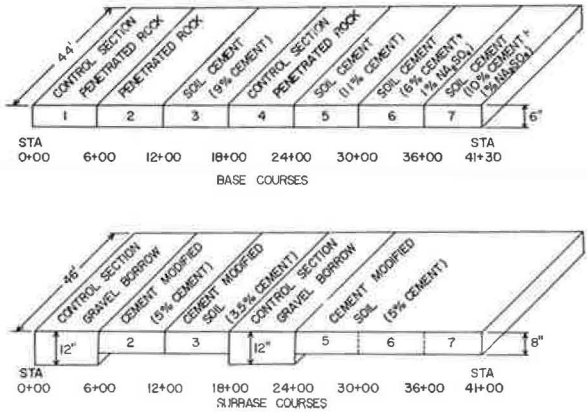

Figure 2. Layout of Benkelman beam deflection test sites.

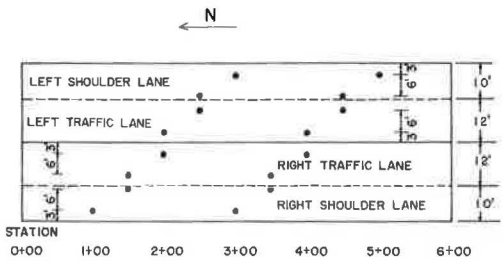

Figure 3. Typical pavement deflection profile from Benkelman beam test on August 1967.

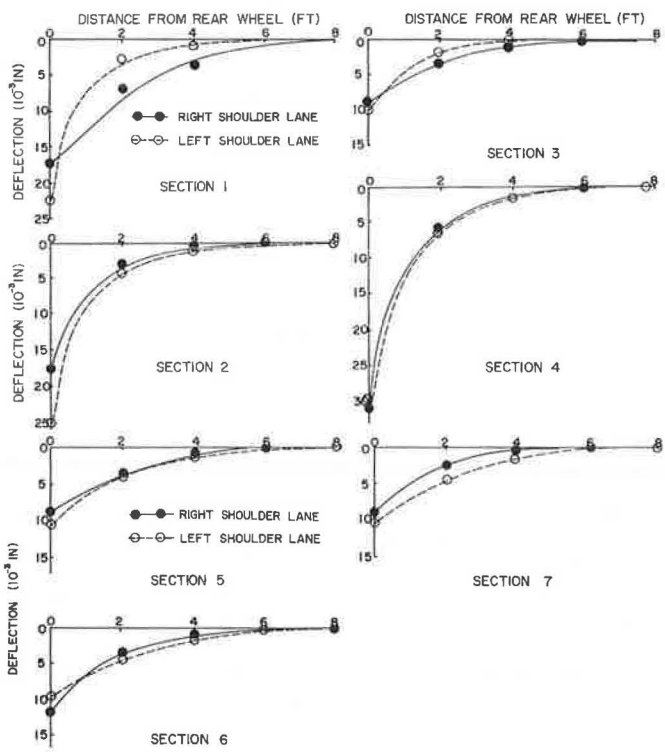

Figure 4. Mean maximum pavement deflection measured in Benkelman beam test.

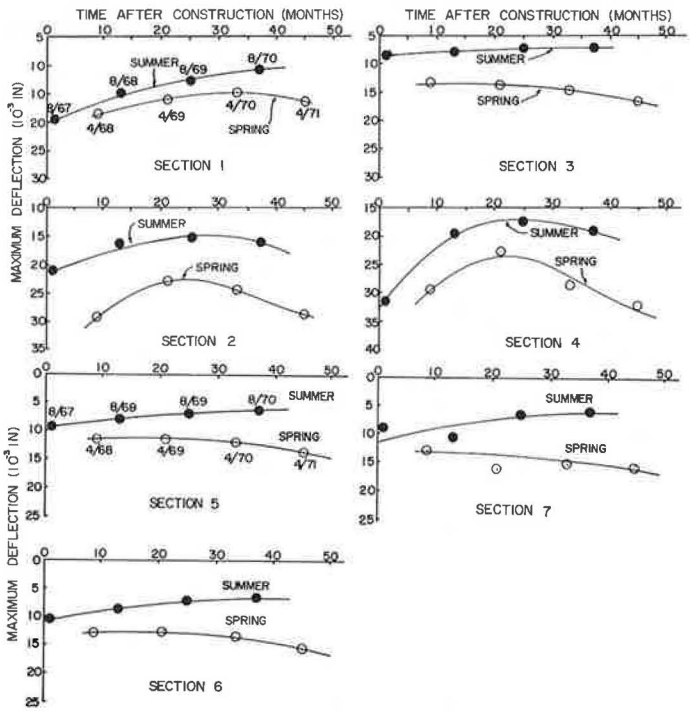

Figure 5. Unconfined compressive strength of base and subbase materials.

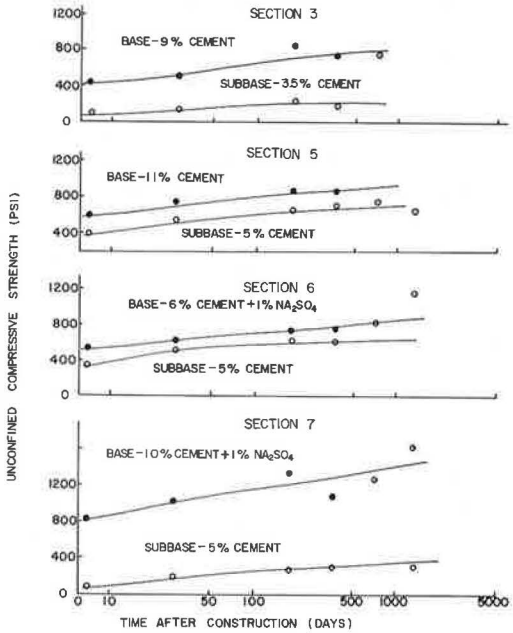

decrease in deflections could be the result of reorientation of particles to a more stable position in the gravel layer due to traffic.

Deflections in sections 2 and 4 first decrease then increase slightly with time. The deflection curve for the spring season illustrates also a tendency of slightly increasing deflection with elapsed time. Factors that could cause an increase in pavement deflection include an increase in subgrade moisture due to precipitation and a deterioration of the pavement material as a result of cracking. The rainfall data (Table 2) indicate a considerably higher rainfall immediately before the Benkelman beam tests conducted in 1970 and 1971. The greater rainfall is presumably the primary cause for the increased deflection shown in Figure 4.

Except for the 2 control sections, 1 and 4, all experimental sections developed cracks. A detailed crack study indicates an increasing amount of cracking with increasing curing time (Fig. 10). Development of cracks could result in an increase in pavement deflection due either to the decrease in load-spreading capacity of the soil-cement layer or to the decrease in load-supporting capacity of subgrade soil because of increasing moisture content caused by the intrusion of surface water through the cracks. The effect of cracking on pavement deflection is given in Table 1. No consistent evidence indicating the destructive effect of cracking is noted from the results obtained to date. Therefore, the tendency of increasing pavement deflection with elapsed time would be primarily caused by the greater rainfall immediately preceding the later tests.

The mean maximum deflection is also shown as a histogram in Figure 6 for easy comparison among sections as follows:

1. The beneficial effect of using a soil-cement base is proved by the fact that the sections with soil-cement bases (sections 3, 5, 6, and 7) exhibit much smaller deflections than those sections having penetrated rock bases (sections 1, 2, and 4).
2. Even though the 2 control sections, 1 and 4, have identical layer thickness, section 4 gives greater deflection then section 1 possibly because of a stronger subgrade support under section 1 (bedrock underlying the pavement was found during excavation).
3. No clear indication of the advantage of substituting an 8-in. thick, 5 percent soil-cement subbase for a 12-in. thick gravel subbase is revealed from the comparison between the deflection in section 2 (with 8-in. 5 percent soil-cement) and deflections in control sections 1 and 4 (with 12-in. gravel) because section 2 deflects as much as section 4 and more than section 1.
4. Regardless of a cement content that is comparatively lower in section 6 (with 6 percent cement plus 1 percent sodium sulfate base) than in section 5 (with 11 percent cement base), section 6 deflects as little as section 5. Both sections contain a 5 percent cement subbase. The addition of 1 percent Na_2SO_4 substantially increases the strength of the cement-stabilized soil. On the contrary, section 7 contains a 10 percent cement plus 1 percent Na_2SO_4 and unexpectedly deflects as much as section 6. A possible reason for this is that the subbase material in section 7 has the same cement content but only about 50 percent of the strength of the material in section 6 (Fig. 5). Because of the effect of unequal subbase support, one can hardly evaluate the advantage of using one material over another in the base course simply from the relative performance in deflection of each pavement section.

Plate Bearing Test

Five different plate load intensities, 5, 10, 15, 20, and 25 kips, were applied statically to a 12-in. diameter plate by using a hydraulic jack. Deflection of the loaded plate was measured at opposite ends of a plate diameter by means of 0.001-in. dial gauges mounted on a reference beam. Two permanent test sites in each section are located on the boundary separating the traffic and shoulder lanes, 150 ft from the beginning of each section on the right and 150 ft from the end on the left.

Tests were conducted annually in different seasons. Results of the test conducted in April 1971 are shown in Figure 7. Each curve represents the average of test results at 2 locations. In general the slope of the load-deflection curves is steeper for the soil-cement sections than for the control sections. The slope of the curve is a function

gure 6. Histogram of mean maximum pavement deflection easured in Benkelman beam tests.

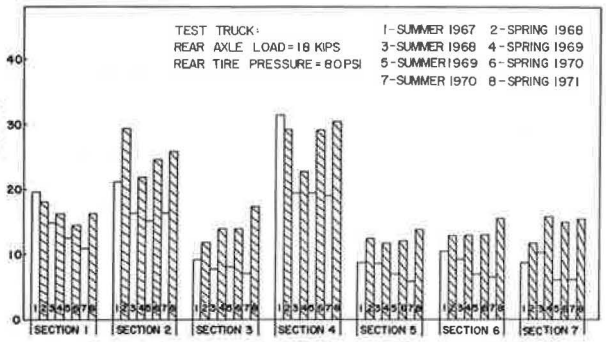

Figure 7. Results of plate bearing test on April 1971.

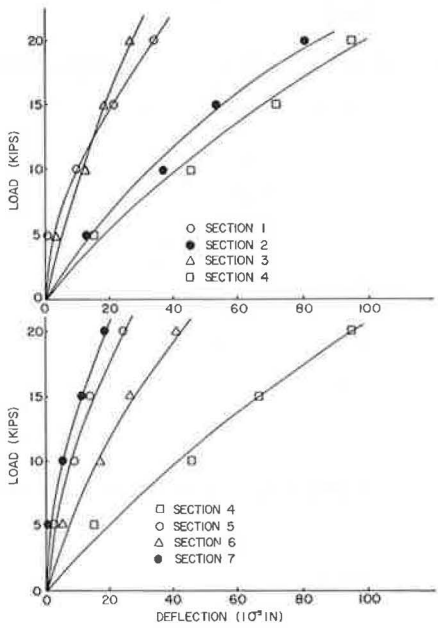

ble 1. Maximum pavement deflection measured in Benkelman beam test.

ction	Station	August 1969 Deflection (10^{-3} in.) Right Shoulder	Right Traffic Lane	Left Shoulder	Left Traffic Lane	April 1971 Deflection (10^{-3} in.) Right Shoulder	Right Traffic Lane	Left Shoulder	Left Traffic Lane
	13+00	0.014				0.040			
	13+50	0.010[a]	0.004[a]			0.013[a]	0.012[a]		
	14+00		0.011		0.007		0.016		0.011
	14+50			0.005[a]	0.006			0.015[a]	0.011[a]
	15+00	0.020		0.008[a]		0.029[a]		0.023[a]	
	15+50	0.006	0.004			0.015[a]	0.013[a]		
	16+00		0.010[a]		0.006[a]		0.019[a]		0.012[a]
	16+50			0.004	0.006			0.009	0.012
	17+00			0.011				0.029	
	25+00	0.009				0.028			
	25+50	0.007	0.007			0.017[a]	0.010[a]		
	26+00		0.008[a]		0.005[a]		0.018[a]		0.012[a]
	26+50			0.004[a]	0.007[a]			0.011[a]	0.015[a]
	27+00	0.011		0.008		0.031		0.019	
	27+50	0.010[a]	0.007[a]			0.018[a]	0.012[a]		
	28+00		0.007[a]		0.006[a]		0.009[a]		0.009[a]
	28+50			0.004	0.005			0.010	0.012
	29+00			0.006[a]				0.022[a]	
	31+00	0.011				0.042[a]			
	31+50	0.009[a]	0.009[a]			0.020[a]	0.017[a]		
	32+00		0.006[a]		0.010		0.008[a]		0.014[a]
	32+50			0.002	0.005[a]			0.011	0.019[a]
	33+00	0.008		0.003		0.031		0.015[a]	
	33+50	0.004	0.008			0.016	0.018		
	34+00		0.008		0.004		0.011		0.012
	34+50			0.005	0.012			0.013	0.012[a]
	35+00			0.008[a]				0.024[a]	
	37+00	0.004			0.008[a]	0.007[a]			0.004[a]
	37+50	0.005[a]	0.013	0.003	0.004	0.015[a]	0.018[a]	0.010	0.011
	38+00		0.010	0.004			0.008	0.020	
	39+00	0.002			0.008	0.037			0.013[a]
	39+50	0.004	0.009	0.006	0.005	0.017[a]	0.026	0.008	0.012
	40+00		0.009[a]	0.004[a]			0.139[a]	0.026[a]	

icks developed around test site.

Table 2. Pavement deflection under 15-kip plate load.

Section	Station	Lane	Deflection (10^{-3} in.) July 1969	Deflection (10^{-3} in.) April 1971
3	13+50	Right	0.017[a]	0.019[a]
	16+50	Left	0.038	0.015[a]
5	25+50	Right	0.029	0.029[a]
	28+50	Left	0.017[a]	0.013
6	31+50	Right	0.024[a]	0.023[a]
	34+50	Left	0.021[a]	0.017[a]
7	37+50	Right	0.011	0.014[a]
	39+50	Left	0.018	0.015

[a]Cracks developed around test sites.

Figure 8. Pavement deflection under 15-kip plate load.

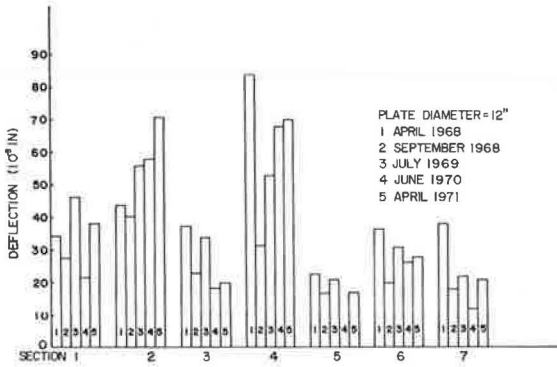

Figure 9. Crack patterns mapped in March 1971.

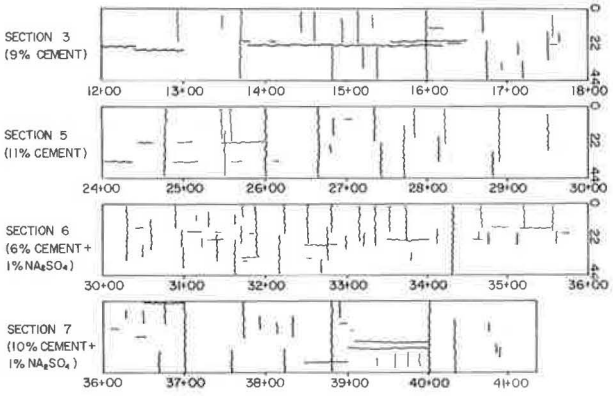

Figure 10. Length of surface crack in test pavements.

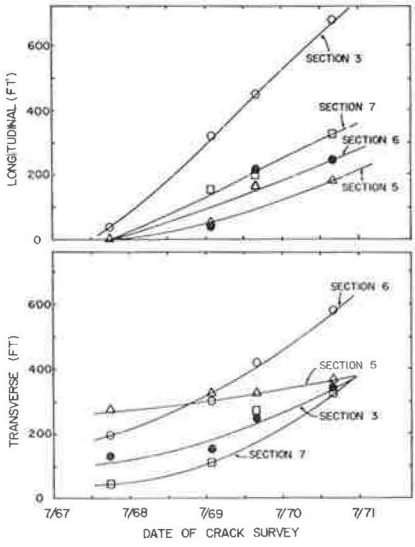

Table 3. Roughometer test results.

Direction	Section	Shoulder Lane Roughness Index (in./mile) May 68	March 69	Oct. 69	Oct. 71	Traffic Lane Roughness Index (in./mile) Aug. 67	May 68	March 69	Oct. 69	Oct. 71
Southbound	1	88	105	89	—	88	79	98	84	—
	2	114	119	119	104	101	88	98	101	113
	3	97	110	99	126	106	92	114	106	121
	4	97	101	98	113	106	92	105	92	110
	5	79	105	95	119	97	92	105	92	117
	6	97	114	107	123	114	101	114	112	121
	7	130	130	121	114	109	115	130	112	115
Northbound	1	97	132	109	—	88	79	114	96	—
	2	105	114	110	115	88	92	105	97	107
	3	79	98	105	124	97	84	105	105	120
	4	97	98	114	115	97	84	98	97	105
	5	88	114	108	121	101	92	98	105	125
	6	97	123	113	103	114	101	114	107	126
	7	120	110	87	105	94	111	120	93	110

of the stiffness of the pavement material; therefore, it is an alternate measure for load-carrying capacity of the pavement sections.

Pavement deflection under a 15-kip plate load is shown in Figure 8. (The intensity of plate load, 15 kips, was selected arbitrarily.) The results follow generally those of the Benkelman beam test. A study of the influence of cracking on pavement deflection under plate loads is given in Table 2. No consistent results indicate that cracking causes an increase in pavement deflection.

Roughometer Tests

The riding quality of the test pavements was determined in terms of a roughness index. Tests were conducted by the Rhode Island Department of Transportation using the BPR roughometer. Three runs on each traffic lane and one on each shoulder lane were made in the tests in August 1967 and May 1968; however, only two runs were made on each traffic lane and one run on each shoulder lane in the tests in March and October 1969 and October 1971. The roughometer was not available for tests in 1970. Test results are given in Table 3.

In general, the surface roughness of shoulder lanes is individually greater than that of traffic lanes for all sections. That condition is presumably caused by either faster traffic or greater confinement effect, or both, in the traffic lane. The faster traffic is, the greater is the impact action, which gives greater smoothing effect; increasing confinement increases pavement stiffness and thus decreases pavement deflection under the test truck. The test results also suggest that control sections 1 and 4 possess smoother surfaces than soil-cement sections. The reason may be that the control sections can be more easily smoothed by traffic than the soil-cement sections can because the penetrated rock base is generally less stiff than the soil-cement base. In addition, as is discussed later, the soil-cement sections develop cracks; cracking disintegrates the pavement and could, therefore, increase pavement roughness.

Cracking Behavior

Surface cracks were first noticed in the winter immediately after completion of construction. Development of cracks was studied by careful surveying and mapping annually. The depths of the cracks were determined by taking core samples across a crack. It was found that the cracks generally go through the entire base course but only to about the middepth of the subbase layer. The widths of the cracks are in general smaller than $\frac{1}{8}$ in., and once cracks developed no further change in width was noted. Cracks were observed in the sections with soil-cement layer only. Thus, the development of surface cracks must be due essentially to the presence of the soil-cement layer.

Surface cracks in the pavement with a soil-cement layer may be a result of thermal stress, cement hydration, stress due to moisture change, non-uniform frost heave, differential settlement, fatigue failure in surface layer or in the soil-cement layer or both, weak bond between two construction strips due to inadequate mixing, and the like. Among all of these possible causes, that of differential frost heave and settlement does not appear likely because neither detectable difference in elevation on either side of cracks nor surface unevenness was observed in surface leveling. In addition, because no alligator cracking developed, the cracking is probably not due to fatigue failure either. Except for some cracks, both transverse and longitudinal, that apparently developed along the construction joint because of inadequate mixing, most cracks are caused by thermal stress, cement hydration, and stress due to moisture change.

The location and length of the cracks observed in March 1971 are shown in Figure 9. All surface cracks develop in transverse and longitudinal directions only. Figure 10 shows the crack length surveyed in April 1969, March 1970, and March 1971. Cracking increases with time for all sections. The length of longitudinal cracking is greatest in section 3 (9 percent cement) and least in section 5 (11 percent cement). Most of the longitudinal cracking in section 3 developed along the centerline of the pavement (Fig. 9). At the beginning, transverse cracks developed the most in section 5 (11 percent cement) and the least in section 7 (10 percent cement plus 1 percent Na_2SO_4). The rate of increase in crack length with time, however, was fastest in section 6 (6 percent ce-

ment plus 1 percent Na_2SO_4) and slowest in section 5. An addition of 1 percent Na_2SO_4 apparently causes an increase in the rate of transverse crack development. Based on the present data, it would appear that section 6 will eventually have the greatest amount of transverse cracking, section 5 will have the least, and sections 7 and 3 will have amounts between these two. More data are needed to lead to a final conclusion, however

Response to Freezing Temperature

In general, the average daily air temperature in the vicinity of the test road reaches a maximum in July and a minimum in January. Freezing temperatures usually occur from December to March. The freezing index and duration of freezing obtained from records of the Newport Water Department are given as follows:

Period	Freezing Index (deg-days)	Duration of Freezing (days)
1967-68	315	62
1968-69	100	32
1969-70	274	44
1970-71	273	53

The response of the test road to freezing temperature was evaluated on the basis of its resistance to the penetration of freezing temperature and the amount of frost heave. Penetration of freezing temperature was determined by using temperature gauges installed in the pavement. No significant frost penetration was detected in the 1968-69 winter because of low freezing index and short duration of freeze. The maximum depth of frost penetration ranged between 14 and 16 in. in the 1967-68 winter and between 8 and 12 in. in the 1969-70 and 1970-71 winters. Unfortunately, conclusions regarding the relative response of each section to frost penetration can hardly be drawn from the data available.

Level of the test road surface was determined by means of an engineer's level at least once a year to detect frost heave. The overall elevation of the pavement surface was higher in the winter than in the summer probably because of the frost action. However, no indication of differential heaving in individual sections and between sections was seen.

SUMMARY AND CONCLUSIONS

Performance of the test road evaluated to date is summarized in the following:

1. At any corresponding elapsed time after construction, the deflections measured by Benkelman beam and plate bearing tests are all greater in the spring than in the summer. Much smaller deflections are yielded by the sections with soil-cement base than by the sections with penetrated rock base (Figs. 6 and 8). The beneficial effect of increasing cement content in the base course, however, is not apparent because of the masking effect due to the weaker subbase in section 7.
2. The surface roughness is generally greater in shoulder lanes than in traffic lanes It seems that the control sections possess a better riding surface than experimental sections (Table 3).
3. All pavement sections with soil-cement bases develop cracks because of thermal stress and cement hydration. The total length of cracks increases with increasing curing time. Results of the crack study seem to suggest that the base course with higher cement content (without Na_2SO_4) develops more transverse cracks at the beginning and the cracks increase with time at a slower rate; furthermore, an addition of 1 percent Na_2SO_4 increases the rate of transverse crack development (Fig. 10). However, more data are required before a final conclusion can be drawn.
4. No significant frost penetration was observed in the 1968-69 winter. The depth of frost penetration varied from 14 to 16 in. in the 1967-68 winter and from 8 to 12 in. in the 1969-70 and 1970-71 winters. The overall surface elevation was higher in the

winter than in the other seasons, and that could be due to frost action. No differential frost heaving in each section and between sections was observed, however.

The pavements constructed with soil-cement base possess greater rigidity and thereby deflect less under loading. With a greater rigidity in the soil-cement layer, the riding quality of the pavements can hardly be improved by the traffic. Furthermore, all soil-cement pavements develop cracks that increase with increasing curing time. Formation of cracks could increase the pavement surface roughness; however, no conclusive evidence to date indicates that cracking would reduce the pavement stiffness and increase surface deflection.

ACKNOWLEDGMENTS

This study was sponsored by the Rhode Island Department of Transportation and the Federal Highway Administration. This support is gratefully acknowledged. The drawings were prepared by Kou R. Chang.

REFERENCES

1. Nacci, V. A., Moultrop, K., and Huston, M. T. Stabilization of Silty Soils With Portland Cement and Sodium Sulfate. Univ. of Rhode Island, Eng. Bull. 9, Aug. 1966.
2. Roderick, G. L. Condition, Postconstruction Report No. 2. July 1968.
3. Initial-Preconstruction Report No. 1. Univ. of Rhode Island, June 1966.
4. Condition-Postconstruction Report No. 1. Univ. of Rhode Island, Oct. 1967.
5. Roderick, G. L., and Huston, M. T. Rhode Island 214 —Soil-Cement Test Section. Highway Research Record 263, 1969, pp. 37-46.

SPONSORSHIP OF THIS RECORD

GROUP 2—DESIGN AND CONSTRUCTION OF TRANSPORTATION FACILITIES
John L. Beaton, California Division of Highways, chairman

Committee on Soil-Portland Cement Stabilization
Earl B. Kinter, Federal Highway Administration, chairman
Mehmet C. Anday, Ara Arman, Sidney Diamond, H. H. Duval, Donald G. Fohs, K. P. George, C. M. Higgins, J. M. Hoover, Ali S. Kemahli, W. A. Lewis, James K. Mitchell, D. F. Noble, Peter Nussbaum, J. Frank Redus, E. Guy Robbins, Marshall R. Thompson, Jerry W. H. Wang, Anwar E. Z. Wissa, Toyotoshi Yamanouchi

John W. Guinnee, Highway Research Board staff